ESD-TR-68-401

ESSX

MTR-743

NARROWBAND INTERFEROMETRY AND THE POLARIZATION SCATTERING MATRIX

H. S. Ostrowsky

DECEMBER 1968

Prepared for

SPACE DEFENSE AND COMMAND SYSTEM PROGRAM OFFICE

ELECTRONIC SYSTEMS DIVISION
AIR FORCE SYSTEMS COMMAND
UNITED STATES AIR FORCE
L. G. Hanscom Field, Bedford, Massachusetts

Project 4966
Prepared by
THE MITRE CORPORATION
Bedford, Massachusetts
Contract AF19(628)-5165

ESD-TR-68-401

MTR-743

NARROWBAND INTERFEROMETRY AND THE POLARIZATION SCATTERING MATRIX

H. S. Ostrowsky

DECEMBER 1968

Prepared for

SPACE DEFENSE AND COMMAND SYSTEM PROGRAM OFFICE

ELECTRONIC SYSTEMS DIVISION
AIR FORCE SYSTEMS COMMAND
UNITED STATES AIR FORCE
L. G. Hanscom Field, Bedford, Massachusetts

Project 4966
Prepared by
THE MITRE CORPORATION
Bedford, Massachusetts
Contract AF19(628)-5165

FOREWORD

This report has been prepared by The MITRE Corporation under Project 4966 of Contract AF 19(628)-5165. The contract is sponsored by the Electronic Systems Division, Air Force Systems Command, L. G. Hanscom Field, Bedford, Massachusetts.

REVIEW AND APPROVAL

This technical report has been reviewed and is approved.

HENRY J. MAZUR, Colonel, USAF
Director, Space Defense & Command Systems Pgm Ofc
Deputy for Surveillance & Control Systems

ABSTRACT

Two previous papers[1][2] have described the concept and some of the applications of Narrowband Interferometry, using monostatic and multistatic radars (at small bistatic angles) to obtain two and three dimensional "images" of targets in terms of their scattering centers. The method involves taking finite Fourier transforms of measured narrowband amplitude and phase data to resolve individual scattering centers in "Doppler" at each radar site.

The present paper extends these methods in two directions. The class of scattering centers considered is widened to include not only isotropic point scatterers as before but also point dipoles, as representatives of orientable scattering centers. The theory is broadened to involve the Polarization Scattering Matrix, so that the polarization behavior of the individual resolved scatterers can be determined as aids to their recognition.

ACKNOWLEDGMENTS

I would like to take this opportunity to say "thanks" to M. R. Weiss, W. J. Riordan, N. M. Tomljanovich, and all the other members of D-85 and D-86 who contributed ideas and moral support during the writing of this paper.

TABLE OF CONTENTS

LIST OF ILLUSTRATIONS

SECTION I
INTRODUCTION

Two previous papers[1][2] have described the concept and some of the applications of Narrowband Interferometry using monostatic and multistatic radars (at small bistatic angles) to obtain two and three dimensional "images" of targets in terms of their scattering centers. The systems therein discussed did not use, nor did the theory refer to, measurements made in more than one polarization. This was sufficient for studying objects composed only of simple isotropic point scattering centers. But real objects do not generally contain many such simple scatterers, and those that do exist are of low cross section compared with other types of scattering centers. In particular, realistic targets are better described in terms of a model which allows for orientable "scatterers", since such things as edges are usually pre-eminent in the scattering-center description of a real object. But, in the case of orientable scattering centers, valuable information is contained in the terms of the complete Polarization Scattering Matrix, which information will be lost if the Scattering Matrix is not utilized.

Now, under ARPA sponsorship, The MITRE Corporation has recently developed and installed a radar system capable of measuring the full scattering matrix on a pulse-by-pulse basis; this system has been integrated into the MITRE-Lincoln Laboratory Tristatic Radar Interferometer. Therefore, the present paper will be devoted to considering what information is present in these scattering matrix measurements and in particular how an appropriate Fourier Transformation of the terms of the scattering

matrix can help to identify the polarization properties of those individual scattering centers which can be resolved in this manner. The theory will be devoted primarily to two types of scattering centers: isotropic point scatterers as simple representatives of non-orientable scattering centers, and point dipole scatterers as simple representatives of orientable scattering centers. Although these idealized scattering centers are in some respects considerable abstractions from the more complicated sorts of scatterers found on real targets, they have the useful property and great advantage of illustrating most of the pertinent geometric properties of the more complex scatterers without the latter's attendent mathematical complexities which obfuscate without enlightening. As a matter of fact, a recent study of the "Doppler Mapping" of an Edge[3] using the methods of the present paper has clearly borne out the contention that the point dipole is a good approximation to the more realistic edge scatterer.

In connection with the term "Doppler Mapping", given in quotation marks in the previous paragraph, I feel that some comments are deserved. The process of taking finite Fourier Transforms of amplitude and phase data in the time domain has been called "Doppler Processing" or "Doppler Mapping" here at MITRE for a long time. The resulting "Doppler Maps" are said to show scattering centers resolved "in Doppler", by which is meant resolution in the f (frequency) domain. But it will become quite apparent, upon careful examination of the analysis given in Section III, that these terms are misnomers. Although the mathematical forms of the

functions obtained are identical to those which are characteristic of the Doppler Effect, the fact is that the terms due to the true Doppler effect are negligible compared to other terms, and drop out of all the equations at an early stage. The effect responsible for the resolution of scattering centers in frequency is due to periodic changes in the phase differences between different scattering centers as these centers move with respect to one another. Nevertheless, the erroneous terms "Doppler Map", etc., have become standard through long usage here at MITRE, and they will continue to be used in this paper, though with quotation marks wherever I could remember to put them in. Whenever quotation marks do not appear on these terms, the reader is asked please to imagine them.

SECTION II

THE POLARIZATION SCATTERING MATRIX

The received signal, in an arbitrary polarization, is related to the transmitted signal, in an arbitrary polarization, through the Polarization Scattering Matrix. The form of the matrix depends on the modes of polarization being used and on the representation employed to describe these modes. We will be concerned here with two different modes, linear and circular. As for the representations, a glance at the literature will show that there is as yet no generally accepted convention, but that the situation is in a state of great confusion. After reading the interesting discussions of the Scattering Matrix to be found in References 4, 5, 6, and 7, and giving great weight to the conventions currently being employed by those directly involved in the ARPA Scattering Matrix Radar Program here at MITRE, and with due regard to the additional requirement that the form of the scattering matrix for a bistatic situation reduce to that for the monostatic case when the bistatic angle goes to zero, I have chosen to define things in what I hope is a reasonable manner. Any differences between the present representation and those found in the above references (aside from those caused merely by the choice of which polarizations are denoted 1 and 2) will be in the signs of the phase factors and should not cause any significant problems.

1. Linear Polarization

Consider a bistatic situation in which a linearly polarized wave is transmitted in direction $\hat{k}$, strikes a target, 0, in the far-field and is reflected toward a receiver in direction $-\hat{k}'$ relative to the target; see Figure 1.

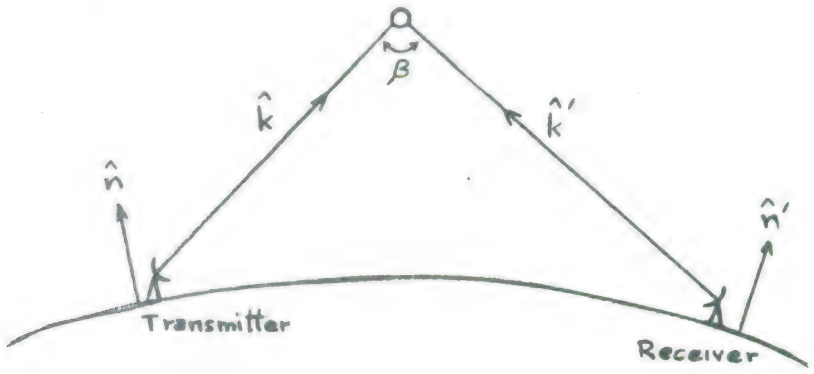

Figure 1. The Bistatic Situation

The bistatic angle, β, is defined by

$$\cos \beta = \hat{k} \cdot \hat{k}' \ ,$$

and unit vectors $\hat{n}$ and $\hat{n}'$ are normals to the earth's surface at the transmitter and receiver respectively.

A plane normal to $\hat{k}$ (or $\hat{k}'$) is called the Transmitter (or Receiver) Polarization plane. In the transmitter polarization plane we may define a unit vector, $\hat{e}_1$, by the equation

$$\hat{e}_1 \equiv \frac{\hat{n} \times \hat{k}}{|\hat{n} \times \hat{k}|} \qquad (2.1a)$$

This vector is clearly "horizontal" according to the usual meaning of the term, and a datum line parallel to this vector in the transmitting antenna plane may be maintained always horizontal however the antenna rotates, thus providing a fixed datum for "horizontal polarization" in transmission. We can now define another unit vector, $\hat{e}_2$, in the transmitter polarization plane, such that $(\hat{e}_1, \hat{e}_2, \hat{k})$ form a right-handed ortho-normal triad:

$$\hat{e}_2 \equiv \hat{k} \times \hat{e}_1 \qquad (2.1b)$$

A datum line parallel to this vector in the transmitting antenna plane is always normal to the "horizontal polarization" datum line and thus provides a fixed datum for what is usually called "vertical polarization" in transmission, even though it is not usually a "vertical" line in the common meaning of that term.

Similarly, to represent the polarization vector of the received signal we choose basis vectors $\hat{e}_1'$ and $\hat{e}_2'$ in the receiver polarization plane:

$$\hat{e}_1' \equiv \frac{\hat{n}' \times \hat{k}'}{|\hat{n}' \times \hat{k}'|} \qquad (2.2a)$$

$$\hat{e}_2 \equiv \hat{k}' \times \hat{e}_1' \qquad (2.2b)$$

Once again, the respective datum lines in the receiving antenna plane provide fixed lines for defining "horizontal" and "vertical" polarization of the received signal. Moreover, the definitions above guarantee that, since $\hat{k}' \to \hat{k}$ and $\hat{n}' \to \hat{n}$ as $\beta \to 0$, these two sets of bases vectors (and lines) have the desired property of becoming identical as $\beta \to 0$.

Now we must exert just a bit of care to define the Scattering Matrix in a way that is valid for both the bistatic and monostatic cases. Suppose the transmitting antenna sends out a unit signal with an arbitrary linear polarization, represented naturally in the unprimed basis as

$$\vec{E}_T \equiv \hat{E}_T \equiv a_1 \hat{e}_1 + a_2 \hat{e}_2 \equiv \begin{pmatrix} a_1 \\ a_2 \end{pmatrix} , \tag{2.3}$$

where $(a_1)^2 + (a_2)^2 = 1$. After striking the target and starting toward the receiver, the returning signal, now represented naturally in the primed basis, may be written as

$$\vec{\mathcal{E}}_R \equiv \mathcal{E}_1 \hat{e}_1' + \mathcal{E}_2 \hat{e}_2' \equiv \begin{pmatrix} \mathcal{E}_1 \\ \mathcal{E}_2 \end{pmatrix} . \tag{2.4}$$

We can now define the scattering Matrix S by requiring that

$$\vec{\mathcal{E}}_R \equiv S \, \vec{E}_T . \tag{2.5}$$

This definition differs from the usual definition of the scattering matrix in that it connects two polarization vectors expressed in <u>different</u> coordinate systems; however, it reduces to the usual definition when $\beta \to 0$.

In order to measure the elements of S, we assume that the receiving antenna is linearly polarized in some direction $\hat{E}_R$ which is represented in the primed basis as

$$\hat{E}_R \equiv a_1'\hat{e}_1' + a_2'\hat{e}_2' \equiv \begin{pmatrix} a_1' \\ a_2' \end{pmatrix} \tag{2.6}$$

where $(a_1')^2 + (a_2')^2 = 1$. Then the signal which is actually received is

$$V \equiv \hat{E}_R \cdot \vec{\mathcal{E}}_R = \hat{E}_R \cdot S\,\hat{E}_T \quad . \tag{2.7}$$

This tells us that in order to measure element S_{ij} of the scattering matrix we must transmit a unit signal with polarization $\hat{e}_j$ and measure the received signal with polarization $\hat{e}_i'$, whereupon the value of the received signal is equivalent to the element S_{ij}.

2. Circular Polarization

It is with circular polarization that the confusion of representation referred to above enters to becloud the picture. We will have to make several definite choices, which will be indicated as we go along. One of these occurs in the definition of "Right Circular" and "Left Circular" polarization. We will not sow confusion by describing the conventions which will NOT be used, but rather will describe only the standard IEEE convention which WILL be used.[8] This convention defines the "handedness" of the circular polarization in terms of the direction of propagation of the signal: A right-circularly polarized wave is one for which the $\vec{E}$-vector rotates in the direction of a right-handed screw as it advances, and conversely for a left-circularly polarized wave. To

put it more graphically, point the thumb in the direction of propagation so that the fingers curl in the direction of rotation of the $\vec{E}$-vector; then the "handedness" of the circular polarization is defined by the physical hand which must be used to accomplish this.

Let us now define a basis for representing circular polarization. The unit vectors $\hat{e}_1$, $\hat{e}_2$, $\hat{k}$ as defined above form a right-handed orthonormal triad, and the same goes for their primed counterparts. Consider a plane wave advancing along the positive $\hat{k}$ direction with polarization vector given by $\hat{e}_1 + i\hat{e}_2$. Of course what we really mean by this is a real wave of the form

$$\vec{E} \equiv \text{Re}\ \{(\hat{e}_1+i\hat{e}_2)e^{i(\vec{k}\cdot\vec{r}-\omega t)}\} \equiv \hat{e}_1\cos(\vec{k}\cdot\vec{r}-\omega t) - \hat{e}_2\sin(\vec{k}\cdot\vec{r}-\omega t).$$

Examining the angle θ between the polarization vector and the $\hat{e}_1$ axis we see that

$$\tan\theta \equiv \frac{\vec{E}\cdot\hat{e}_2}{\vec{E}\cdot\hat{e}_1} = \frac{-\sin(\vec{k}\cdot\vec{r}-\omega t)}{\cos(\vec{k}\cdot\vec{r}-\omega t)} = \tan(\omega t-\vec{k}\cdot\vec{r})$$

whence

$$\theta(\vec{r},t) = \omega t-\vec{k}\cdot\vec{r} \quad ;$$

this shows that as a function of t the polarization vector is advancing and turning in the same way as a right-handed screw.

Next let us consider a plane wave advancing along the $(-\hat{k})$ direction with the same polarization vector $\hat{e}_1 + i\hat{e}_2$. In this case what is meant is a real wave of the form

$$\vec{E} \equiv \text{Re}\ \{(\hat{e}_1+i\hat{e}_2)e^{i(\vec{k}\cdot\vec{r}+\omega t)}\} \equiv \hat{e}_1\cos(\vec{k}\cdot\vec{r}+\omega t) - \hat{e}_2\sin(\vec{k}\cdot\vec{r}+\omega t),$$

whereupon the angle θ between the polarization vector and the $\hat{e}_1$ axis becomes

$$\theta(\vec{r},t) = -\omega t-\vec{k}\cdot\vec{r} \quad .$$

Since the wave is propagating in the direction $(-\hat{k})$, this shows that as a function of t the polarization vector is again advancing and turning in the same way as a right-handed screw.

Thus we have seen that the complex polarization vector $\hat{e}_1+i\hat{e}_2$ always represents a right-circularly polarized wave, both in transmission and reflection. Similarly, we could show that the complex polarization vector $\hat{e}_1-i\hat{e}_2$ always represents a left-circularly polarized wave. Therefore we define, as basis vectors for representing circular polarization, the complex vectors $\hat{C}_1$ and $\hat{C}_2$ which in the linear basis have the representations

$$\sqrt{2}\ \hat{C}_1 \equiv \hat{e}_1 + i\hat{e}_2 \equiv \begin{bmatrix} 1 \\ i \end{bmatrix} : \quad \text{R.H.C.} \qquad (2.8a)$$

$$\sqrt{2}\ \hat{C}_2 \equiv \hat{e}_1 - i\hat{e}_2 \equiv \begin{bmatrix} 1 \\ -i \end{bmatrix} : \quad \text{L.H.C.} \qquad (2.8b)$$

A similiar basis is defined for the primed coordinate system.

A word about normalization may be in order here. Because they are complex, the vectors $\hat{C}_j$ cannot be normalized in the usual dot product sense. Instead we must use the Hermitian scalar product of the form

$$< \vec{u}, \vec{v} > \equiv \vec{u} \cdot \vec{v}^{\,*} \ ,$$

whereupon we see that

$$< \hat{C}_i , \hat{C}_j > = \delta_{ij} \ .$$

But actually it will not be necessary to use this form of normalization in the analyses to follow; in use the $\hat{C}_j$ always appear multiplying a "phase factor" of the form $e^{i(\vec{k}\cdot\vec{r} \pm \omega t)}$ with the Real Part of the product being understood to be taken. When this has been done, the resulting vectors will be found to be properly normalized in the ordinary sense, so no more need be thought about it.

Let us now proceed to transform the scattering matrix from its representation in the linear bases, S, to its representation in the circular bases, which we will denote by C . Let Λ be the matrix that transforms a vector from the circular basis to the linear one; using eqns. (2.8) it is easily seen that

$$\Lambda \equiv \frac{1}{\sqrt{2}} \begin{bmatrix} 1 & 1 \\ i & -i \end{bmatrix} \qquad (2.9)$$

Now we rewrite eq. (2.7) in the form

$$V = \tilde{E}_R(e')\ S\ E_T(e), \tag{2.10}$$

where the argument e' or e refers to the primed or unprimed linear basis and the tilda ($\sim$) indicates the transpose of a vector or matrix . In an obvious notation,

$$E_R(e') \equiv \Lambda\, E_R(c') \text{ and } E_T(e) \equiv \Lambda\, E_T(c) ,$$

so eq. (2.10) becomes

$$V = \tilde{E}_R(c')\tilde{\Lambda}\, S\Lambda\, E_T(c) . \tag{2.11}$$

But the scattering matrix C is defined, analogously to the definition of S, by the identity

$$V \equiv \hat{E}_R(c')\cdot\ C\ \hat{E}_T\ (c) , \tag{2.12}$$

whereupon we see that

$$C \equiv \tilde{\Lambda}\, S\, \Lambda \tag{2.13}$$

A little matrix multiplication now yields the elements of C:

$$
\begin{aligned}
2C_{11} &= (S_{11} - S_{22}) + i(S_{12} + S_{21}) \\
2C_{12} &= (S_{11} + S_{22}) - i(S_{12} - S_{21}) \\
2C_{21} &= (S_{11} + S_{22}) + i(S_{12} - S_{21}) \\
2C_{22} &= (S_{11} - S_{22}) - i(S_{12} + S_{21})
\end{aligned}
\tag{2.14}
$$

We should also consider the effect of Faraday rotation, which takes a simple form in the circular representation. Faraday rotation is due to an anisotropy of the ionosphere which causes the propagation constant for an electromagnetic wave to be slightly different according to the sense of circular polarization of the wave traversing the medium.[4] The result is that one component gains in phase proportional to the distance traversed, and the other component loses an equal amount of phase. The discussion of this subject in Reference 4 is very clear and need not be repeated here; the net result is that the scattering matrix C has additional phase factors in the off-diagonal terms, Viz:

$$
C = \begin{bmatrix} C_{11} & C_{12}e^{+i2\psi} \\ C_{21}e^{-i2\psi} & C_{22} \end{bmatrix} \tag{2.15}
$$

where ψ , the amount of one-way Faraday rotation, is proportional to the distance between the radar and the target. Although it varies with time

of day, the sunspot cycle, etc., the value of ψ for a traversal of the entire ionosphere has not exceeded 30^{o} in measurements made at MITRE[10]; it is generally a rather slowly varying function of distance and time.

SECTION III

THE SCATTERING CENTER MODEL

In this paper we adopt the model whereby the scattering from an object is presumed to be explained in terms of a relatively small number of isolated scattering centers of various sorts; the description of the object then consists of determining the locations and properties of its constituant scattering centers. Some of these scattering centers (e.g. point scatterers) are assumed to be rigidly attached to the center of rotation of the object, so that a study of the motions of these scatterers enables one to determine the gross body motion of the object itself. Others (e.g. edges) are only in part rigidly connected to the object center, being capable of "sliding" along a space curve as the object rotates; such scatterers are rather more difficult to deal with, and provide less direct information about the gross body motion.[3] Yet another type of scattering "center", the specular, is slippery in two dimensions, being capable of "sliding" along a surface in space as the object rotates; this type partakes so little of the characteristic of localizability that perhaps it ought to be excluded from the class of "scattering centers" altogether.

The scattering center model of an object has been in use for quite some time, and it has been employed in numerous problems. It appears to be the only convenient way to deal with the subject of the present paper, and it will be used herein. But, though this is not the time or place for a critical review of the concept, a serious caveat is definitely called-for. The model must be understood in its context as a high frequency

approximation, that is, that the object being studied and in fact the individual scattering centers themselves are large compared with the wave-length. In this context it makes little sense to speak of small isotropic "point" scatterers: the nearest thing to a true rigidly-attached point scatterer is a tip, which is approximately isotropic but is very low in reflecting power; on the other hand, the only sizeable truely isotropic scattering center is a specular, which also most resembles a "point" but is far from being rigidly attached. All the other types of scattering centers are also more or less idealizations of the true situation. The most realistic is the edge, which also probably makes up the class of scatterers most prevalent in objects other than smooth ellipsoids.

What is one to infer from all this? We must deal with a mathematically tractable model, or else the complexities of the solution will obscure the simple physical realities which are being presented. So we will use isotropic point scatterers, and we will represent orientable scatterers (such as edges) primarily by the fiction of point dipoles, and we will touch on real edges only a slight bit (though in fact their properties seem to be well represented in terms of point dipoles that can "slip"), but we will also keep in mind that these are <u>models</u>, whose only true test of validity is this: does it help to explain the experimental observations? To the extent that it does, the model (however unrealistic) is justified; to the extent that it does not, we must seek for a more reasonable model.

With this understanding, then, let us describe the scattering center model and its relationship with the radar system, and consider carefully

what happens as a transmitted radar signal strikes the target and returns to the receiving antenna. We assume that the target is composed of a finite (and relatively small) number of scattering centers of various kinds, all connected in some way to a center of mass 0 which is being translated with velocity $\vec{V}(t)$. The target is supposed to be rotating about 0 as a rigid body with angular velocity $\vec{\omega}(t)$. Some of the scattering centers (such as the idealized isotropic point scatterers and point dipoles) are assumed to be rigidly connected to the center of mass and therefore partake fully of the rigid rotation $\vec{\omega}$. Others (such as edges and speculars) must be visualized as slipping along a space curve or a surface and hence partake only in part of the rigid-body rotation. But all of them, whether slippery or not, may be assumed to be located at a particular point at each instant of time, given by $\vec{r}_n(t)$ with respect to 0.

This target is being tracked by a radar interferometer consisting of a narrowband transmitter-receiver located at A and remote receivers located at B and C; the angle subtended at the target by the interferometer is assumed to be small. It is further assumed that the transmitter is capable of transmitting and each receiver is capable of receiving signals of two orthogonal polarizations, and each receiver can measure both amplitude and phase in each polarization channel. The radar operates at frequency f_o and transmits pulses of length Δ seconds, where for concreteness in visualization we may use values like those of the present MITRE-Lincoln Laboratory Interferometer, i.e.,

$$f_o \simeq 10^3 \text{ MHz and } \Delta \simeq 1 \text{ ms} .$$

Referring to Figure 2, the line-of-sight vectors from radars A, B, C, to target center 0 are respectively $\vec{R}_A$, $\vec{R}_B$, $\vec{R}_C$. For all reasonable satellite objects and passes the following set of conditions will easily obtain:

1. The target is very small compared with its distance from the radars; in fact

$$\frac{\max \{|\vec{r}_n - \vec{r}_m|\}}{\min \{R\}} < 10^{-4} .$$

2. The target is very small compared with the length of the radar pulse in space; in fact

$$\frac{\max \{|\vec{r}_n - \vec{r}_m|\}}{c\ \Delta} < 10^{-4} .$$

3. The bistatic angle at the target between any pair of radars is small; in fact

$$\beta \sim D/R \lesssim 10^{-1} \text{ radians.}$$

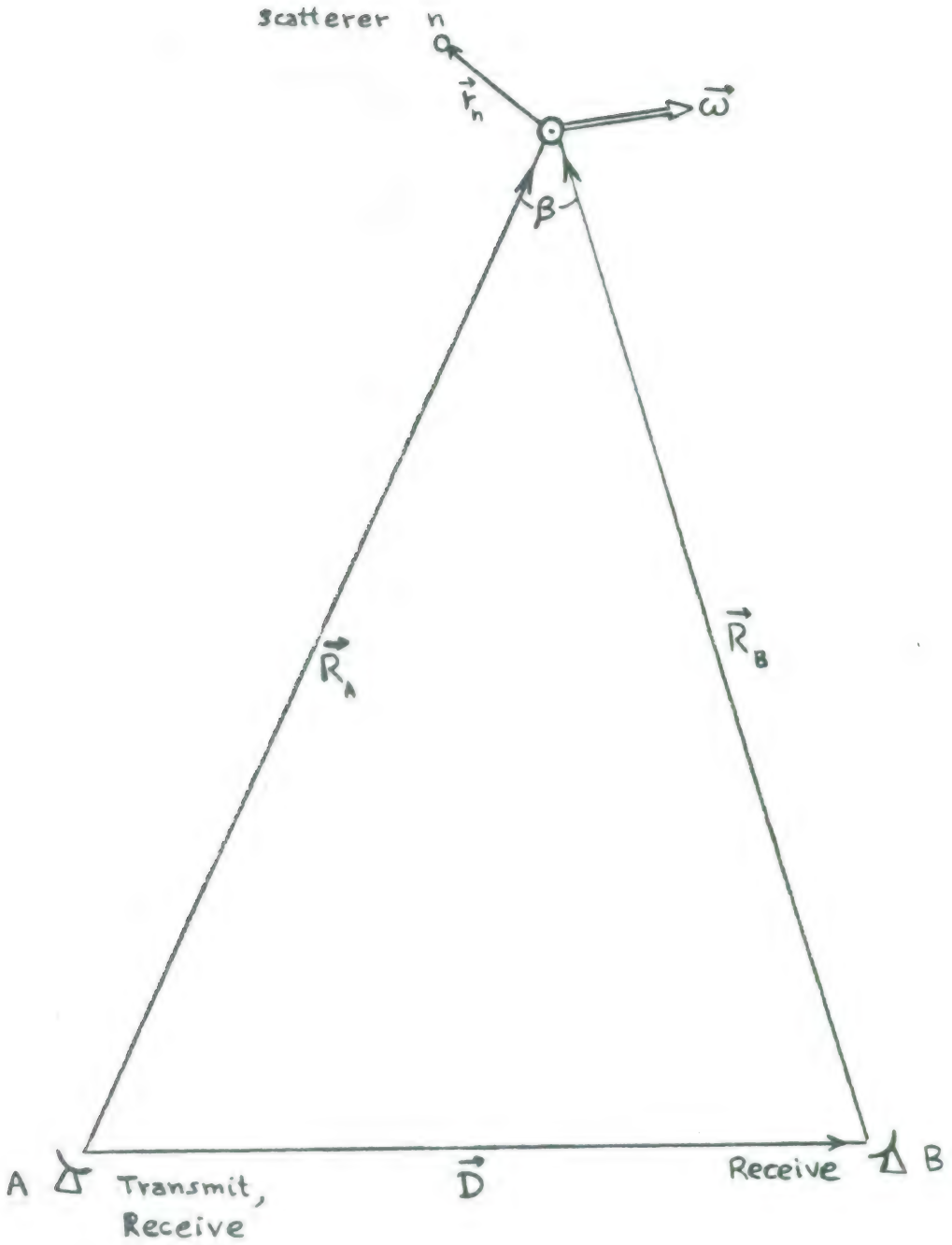

Figure 2. Geometry for a Two-Site Interferometer (not to scale).

Now assume that at time t_o antenna A transmits a pulse, of polarization $\hat{E}_T$, toward the target. Conditions 1 and 2 above allow us to make the far field approximation whereby the transmitted pulse as it approaches scattering center n may be considered to be of the form,

$$\vec{E}_n \sim \hat{E}_T \frac{e^{i\phi_o}}{R_A} \exp\{2\pi i \frac{f_n}{c} [(R_A + \hat{R}_A \cdot \vec{r}_n) - c(t-t_o)]\} , \quad (3.1)$$

where

$$f_n \simeq f_o[1 - \frac{1}{c} \vec{V}\cdot\hat{R}_A - \frac{1}{c} \hat{R}_A \cdot \vec{\omega}_n \times \vec{r}_n] \quad (3.2)$$

represents the Doppler-shifted frequency of the incoming wave relative to the scatterer; here $\vec{\omega}_n$ is the effective angular velocity of the scatterer taking into account any slipperiness: for rigidly attached isotropic points and point dipoles $\vec{\omega}_n \equiv \vec{\omega}$. In writing eq. (3.1) we have ignored a term of order r_n/R_A in the denominator and also ignored a difference in angle of the order of r_n/R_A in the polarization vector at the location of scatterer n relative to $\hat{E}_T$(incident at 0); both of these approximations are of course well justified by condition 1. The use of a monochromatic spherical wave for the incident pulse near the target is justified by condition 2.

Notice that the incident wave front reaches each scatterer n at location $x_n \equiv R_A + \hat{R}_A \cdot \vec{r}_n$ at time $t_n = t_o + \frac{x_n}{c}$, whereupon eq. (3.1) tells us that

$$\vec{E}_n \sim E_T \, e^{i\phi_o/R_A}$$

at each scattering center at the instant it begins to be excited by the incident pulse. The effect of the scattering center on the incident pulse will be symbolically represented by the operator σ, so that the wave which the scattering center begins to re-radiate has the form $\sigma\hat{E}_T e^{i\phi_o/R_A}$ at the instant when re-radiation begins. The form of the operator σ will of course depend on the nature of the scattering center involved. In re-radiation two cases must now be distinguished.

CASE I. RE-RADIATION BACK IN THE DIRECTION OF TRANSMITTER A.

The wave re-radiated by scattering center n goes in the direction $-\hat{R}_A$. The Doppler shift causes an additional change of frequency such that the new frequency is

$$f_n^A \simeq f_o\left[1 - \frac{2}{c}\vec{V} \cdot \hat{R}_A - \frac{2}{c}\hat{R}_A \cdot \vec{\omega}_n \times \vec{r}_n\right] . \qquad (3.3)$$

Now as it approaches the receiver at A the re-radiated signal wave front has the form

$$\vec{E}_n^A \sim \sigma \hat{E}_T \frac{e^{i\phi_o}}{R_A^2} \exp\left\{2\pi i \frac{f_n^A}{c}\left[- R_A - \hat{R}_A \cdot \vec{r}_n + c(t-t_n)\right]\right\}$$

Here t is the nominal time of arrival of the re-radiated wave front from the center of the target at 0, given by $t = t_o + 2R_A/c$; we use this nominal time so that we can later sum the contributions from all the scattering centers at the same instant of reception. With this value of t the received signal from scatterer n appears as

$$\vec{E}_n^A \sim \frac{1}{R_A^2} \sigma \hat{E}_T e^{i\phi_o} \exp\left[-4\pi i \frac{f_n^A}{c} (\hat{R}_A \cdot \vec{r}_n)\right] \quad . \tag{3.4}$$

Using eq. (3.3) the bracketed phase factor in eq. (3.4) can be written as

$$\phi = \frac{-4\pi}{\lambda_o} \hat{R}_A \cdot \vec{r}_n \left[1 - \frac{2}{c} \vec{V} \cdot \hat{R}_A + \frac{2}{c} \hat{R}_A \times \vec{r}_n \cdot \vec{\omega}_n\right] \quad .$$

But for reasonable objects and passes $r_n < 10\text{m.}$, $\omega_n < 1$ rad/sec, and $V \sim 10^4$m/sec, whereupon

$$\left| \frac{2}{c} \vec{V} \cdot \hat{R}_A \right| < 10^{-4}$$

and

$$\left| \frac{2}{c} \hat{R}_A \times \vec{r}_n \cdot \vec{\omega}_n \right| < 10^{-7} \quad .$$

This means that even when multiplying the factor $\frac{4\pi}{\lambda_o} \hat{R}_A \cdot \vec{r}_n$ these two terms contribute no more than about 3^o to the phase, and we shall neglect them in comparison with the first term. Then we may write the received signal from scattering center n as

$$\vec{E}_n^A \sim \frac{e^{i\phi_o}}{R_A^2} \sigma \hat{E}_T \exp\left[\frac{-4\pi i}{\lambda_o} \hat{R}_A \cdot \vec{r}_n\right] .$$

If the receiving antenna is polarized in direction $\hat{E}_R^A$ [where $\hat{E}_R^A \cdot \hat{R}_A = 0$] then the received signal from scatterer n has the form

$$E_n^A \sim \frac{e^{i\phi_o}}{R_A^2} \hat{E}_R^A \cdot \sigma \hat{E}_T \exp\left[-\frac{4\pi}{\lambda_o} i\hat{R}_A \cdot \vec{r}_n\right] . \qquad (3.5)$$

There is nothing unexpected about this result, but in the first place it demonstrates that there is no direct effect from the Doppler shift on the phase of the signal received, and in the second place it shows how to proceed in the less obvious bistatic case to be considered next.

CASE II. RE-RADIATION IN THE DIRECTION OF REMOTE RECEIVER B.

The wave re-radiated by scattering center n goes in the direction $-\hat{R}_B$. The Doppler shift causes an additional change of frequency such that the new frequency is

$$f_n^B \simeq f_o \left[1 - \frac{1}{c} \vec{V} \cdot (\hat{R}_A + \hat{R}_B) - \frac{1}{c} (\hat{R}_A + \hat{R}_B) \cdot \vec{\omega}_n \times \vec{r}_n\right] .$$

Now we define

$$\hat{R}_{AB} \equiv \frac{\hat{R}_A + \hat{R}_B}{|\hat{R}_A + \hat{R}_B|} \tag{3.6}$$

and

$$\cos \beta \equiv \hat{R}_A \cdot \hat{R}_B \ , \tag{3.7}$$

whereupon it is easily seen that

$$R_A + R_B \equiv 2R_{AB} \cos \left(\frac{\beta}{2}\right) \ , \tag{3.8}$$

and the Doppler-shifted frequency is

$$f_n^B \simeq f_o \left[1 - \frac{2}{c} \vec{V} \cdot \hat{R}_{AB} \cos \left(\frac{\beta}{2}\right) - \frac{2}{c} \hat{R}_{AB} \cdot \vec{\omega}_n \times \vec{r}_n \cos \left(\frac{\beta}{2}\right)\right] .$$

However, just as in Case I we may drop the last two terms in the bracket as being quite negligible in comparison with the first term, leaving simply

$$f_n^B \simeq f_o \ .$$

Proceeding further as in Case I we find the signal re-radiated by scatterer n to be, in the far field near receiver B,

$$\vec{E}^{B}_{n} \sim \sigma' \, \hat{E}_T \, \frac{e^{i\phi_o}}{R_A R_B} \, \exp\{2\pi i \frac{f_o}{c} [- R_B - \hat{R}_B \cdot \vec{r}_n + c(t-t_n)]\},$$

with t being the nominal time of arrival of the re-radiated wave front from 0: $t \equiv t_o + \frac{1}{c}(R_A + R_B)$. Here σ' is the operator, corresponding to σ in Case I, representing symbolically the effect of the scattering center on the incident pulse for re-radiation in the primed direction; σ' may or may not be the same as σ, depending on the nature of the scattering center involved. Using eq. (3.8) and the value of t given above, the received signal B becomes

$$\vec{E}^{B}_{n} \sim \frac{e^{i\phi_o}}{R_A R_B} \, \sigma' \, \hat{E}_T \, \exp\left[- \frac{4\pi}{\lambda_o} \, i \, \hat{R}_{AB} \cdot \vec{r}_n \cos\left(\frac{\beta}{2}\right)\right].$$

If the receiving antenna is polarized in direction $\hat{E}^{B}_{R}$ [where $\hat{E}^{B}_{R} \cdot \hat{R}_B = 0$] then the received signal from scatterer n has the form

$$E^{B}_{n} \sim \frac{e^{i\phi_o}}{R_A R_B} \, \hat{E}^{B}_{R} \cdot \sigma' \, \hat{E}_T \exp\left[- \frac{4\pi}{\lambda_o} \, i\hat{R}_{AB} \cdot \vec{r}_n \cos\left(\frac{\beta}{2}\right)\right] \qquad (3.9)$$

A similar analysis can of course be done for remote receiver C also; the result is like eq. (3.9) with B everywhere replaced by C and with $\cos\beta \equiv \hat{R}_A \cdot \hat{R}_C$.

After reception the return signals are compared with a reference signal for phase, which has the effect of eliminating the phase factor ϕ_o but inserting a "range-phase" factor which has the form $4\pi R_A/\lambda_o$

in the monostatic case and $2\pi(R_A + R_B)/\lambda_o$ in the bistatic case. During the course of the data processing, however, very accurate determinations of range are made, which allow the range-phase factor to be removed and also permit the recorded signal amplitudes to be compensated for the $1/R_A^2$ or $1/R_A R_B$ dependence thereby transforming the results into absolute units. In the remaining sections of this paper it will be taken for granted that both of these processing steps have been done.

SECTION IV

ISOTROPIC POINT SCATTERERS

The term "isotropic point scatterer" will be used here to refer to any scattering center, whatever its nature, which satisfies the following criteria.

1. The scattering center can be represented as a point rigidly attached, by a vector $\vec{r}_n(t)$, to the object's center of mass, 0, and rigidly rotating about 0 with the object's angular velocity $\vec{\omega}(t)$. The magnitude, r_n, of the vector $\vec{r}_n$ is a constant, independent of t.

2. In the linear polarization, the scattered wave has the same polarization as the incident wave; i.e., there is no depolarization. This is assumed to be true both for the monostatic case (back-scattering) and for the bistatic case for at least the small bistatic angles considered here.

3. The scattering is characterized by a complex number, the scattering coefficient, of the form $H_n e^{i\Psi_n}$, where H_n gives the relative strength of the re-radiated signal and Ψ_n gives the phase change (if any) upon re-radiation. The numbers H_n and Ψ_n may differ from one scattering center to another, but they are constant in time and angle.

Suppose now that a unit signal is transmitted with linear polarization $\hat{E}_T \equiv \hat{e}_j$. By our assumptions above, the effect of scatterer n on this signal will be represented (in either the monostatic or the bistatic case) by

$$\sigma\hat{E}_T \equiv \sigma'\hat{E}_T = \hat{e}_j H_n e^{i\Psi_n} \tag{4.1}$$

Thus, distinguishing between the monostatic and the bistatic cases, if the receiving antenna has linear polarization given by

$$\text{(monostatic):} \qquad \hat{E}_R^A \equiv \hat{e}_i$$

$$\text{(bistatic)} : \qquad \hat{E}_R^B \equiv \hat{e}_i' \quad , \tag{4.2}$$

then the received signal is characterized by

$$\text{(monostatic):} \qquad \hat{E}_R^A \cdot \sigma\hat{E}_T = \hat{e}_i \cdot \hat{e}_j H_n e^{i\Psi_n} \tag{4.3a}$$

$$\text{(bistatic)} : \qquad \hat{E}_R^B \cdot \sigma'\hat{E}_T = \hat{e}_i' \cdot \hat{e}_j H_n e^{i\Psi_n} \tag{4.3b}$$

Making use now of Eq. (3.5), the comment at the end of section III, the definition of Scattering Matrix, and the fact that $\hat{e}_i \cdot \hat{e}_j \equiv \delta_{ij}$, we see that in the linear basis and for the monostatic case the scattering matrix for the n^{th} scatterer has the elements

$$\text{(monostatic):} \qquad S_{ij} = \delta_{ij} H_n e^{i\Psi_n} \exp[-4\pi i \frac{r_n}{\lambda_o} \hat{R}_A \cdot \hat{r}_n]. \tag{4.5}$$

For the bistatic case the situation is made somewhat more complicated by the presence of the matrix $\hat{e}'_i \cdot \hat{e}_j$ which is not simply equal to δ_{ij}. However, for small bistatic angles it can be shown (see Appendix A) that

$$\hat{e}'_j \cdot \hat{e}_j \simeq \delta_{ij} - (\frac{\beta}{2})^2 K_{ij} \tag{4.5}$$

where the matrix K has elements of order unity. Therefore if we make use of Eq. (3.9) and ignore terms of order $(\frac{\beta}{2})^2$, we see that in the linear basis and for the bistatic case the scattering matrix for the n^{th} scatterer has the elements

$$\text{(bistatic):}\quad S_{ij} \simeq \delta_{ij} H_n e^{i\Psi_n} \exp[-4\pi i \frac{r_n}{\lambda_o} \hat{R}_{AB} \cdot \hat{r}_n \cos(\frac{\beta}{2})] \ . \tag{4.6}$$

Here we have retained the factor $\cos(\frac{\beta}{2})$ in the exponent, even though it is approximately equal to $1 - \frac{1}{2}(\frac{\beta}{2})^2$, because it appears multiplied by what may be a large number (i.e. $4\pi\ r_n/\lambda_o$) and phase factors are always taken modulo 2π so this may make a significant difference.

Transforming into the circular basis by means of Eq. (2.14), we find that the scattering matrix for the n^{th} scattering center has the elements

$$\text{(monostatic):}\quad C_{ij} = (1 - \delta_{ij}) H_n e^{i\Psi_n} \exp[-4\pi i \frac{r_n}{\lambda_o} \hat{R}_A \cdot \hat{r}_n], \tag{4.7}$$

$$\text{(bistatic):}\quad C_{ij} \simeq (1 - \delta_{ij}) H_n e^{i\Psi_n} \exp[-4\pi i \frac{r_n}{\lambda_o} \hat{R}_{AB} \cdot \hat{r}_n \cos(\frac{\beta}{2})]. \tag{4.8}$$

These values of the scattering matrix elements are for one pulse only. It will now be necessary to find expressions for the time-dependence of the C_{ij} . Since, by the defining properties stated previously, the quantities H_n, Ψ_n, and r_n are constants, the only functions which can contain the time dependence of C are $\hat{R}_A \cdot \hat{r}_n$ in Eq. (4.7) and $\hat{R}_{AB} \cdot \hat{r}_n \cos(\frac{\beta}{2})$ in Eq. (4.8). Let us examine them further in this regard.

We will eventually need to take the finite Fourier Transform of the elements $C_{ij}(t)$, integrating over a time interval of length T centered on some time t_o: $t_o - \frac{T}{2} \leq t \leq t_o + \frac{T}{2}$. Usually T will be "small," the precise meaning of which will become clear as we proceed. Therefore we will expand all time-dependent functions in Taylor series about t_o and keep only first-order terms in small quantities.*

For $\hat{r}_n(t)$ we note that $\frac{d\hat{r}_n}{dt} = \vec{\omega}(t) \times \hat{r}_n(t)$, whereupon the Taylor Series gives

$$\hat{r}_n(t) \simeq \hat{r}_n(t_o) + (t-t_o)\, \vec{\omega}(t_o) \times \hat{r}_n(t_o) + O\,(\omega \tfrac{T}{2})^2 \quad . \qquad (4.9)$$

In order for this linearization to be valid, it is necessary that $(\omega \frac{T}{2})^2 \ll 1$ hold true. To be concrete, suppose we require that $\omega\, T/2 < 0.1$. Then writing $\omega \equiv 2\pi/\tau$, where τ is the period of the object's rotation, this condition becomes approximately

---

*For certain purposes it may be useful to retain the second-order terms also, but this will not be considered in the present paper.

$$T \lesssim 0.03\ \tau \quad . \tag{4.10}$$

This may be regarded physically as a limitation on the length of the integration interval T in comparison with the body rotation period τ, such that the Fourier Transform not be "smeared-out" by rotation through too large an aspect angle during the integration. If amplitude weighting is used during integration to reduce the contributions of data points near the ends of the interval ($|t-t_o| \sim \frac{T}{2}$) in comparison with data points near the center, then presumably this condition may be relaxed a bit. How much, depends on the form of weighting used; perhaps $T \lesssim 0.05\ \tau$ would be alright.

The function $\hat{R}_A(t)$ varies quite slowly under most conditions; if we write

$$\frac{d}{dt}\ \hat{R}_A \equiv \vec{\omega}_A(t) \times \hat{R}_A(t),$$

then $\omega_A \lesssim 10^{-2}$ rad/sec except near zero-Doppler of very close passes. Furthermore, $\vec{\omega}_A$ itself changes quite slowly, so that it is reasonable to assume that $\frac{d}{dt}\ \vec{\omega}_A \approx 0$ for $t_o - \frac{T}{2} \le t \le t_o + \frac{T}{2}$ even if T is not absolutely small. Therefore we can approximate $\hat{R}_A(t)$ by the first two terms of its Taylor Series expansion:

$$\hat{R}_A(t) \simeq \hat{R}_A(t_o) + (t-t_o)\ \vec{\omega}_A(t_o) \times \hat{R}_A(t_o) + O(\omega_A \tfrac{T}{2})^2 \quad . \tag{4.11}$$

For the bistatic case, if we write

$$\frac{d}{dt}\left[\hat{R}_{AB}\cos\left(\frac{\beta}{2}\right)\right] \equiv \vec{\omega}_{AB}(t) \times \hat{R}_{AB}(t)$$

and make use of Eq. (3.8) to express $\hat{R}_{AB}\cos\left(\frac{\beta}{2}\right)$ in terms of $\hat{R}_A$ and $\hat{R}_B$, then it turns out that the difference between $\vec{\omega}_{AB}$ and $\vec{\omega}_A$ is of second order in small quantities. Therefore we can write, analogously to Eq. (4.11),

$$\hat{R}_{AB}(t) \simeq \hat{R}_{AB}(t_o) + (t-t_o)\,\vec{\omega}_A(t_o) \times \hat{R}_{AB}(t) + O(\omega_A \tfrac{T}{2})^2 . \qquad (4.12)$$

Substituting Eqn.s (4.9) and (4.11) into (4.7) leads to the following expressions for the time dependence of the scattering matrix elements for the n^{th} scattering center in the monostatic case:

$$C^M_{ij}(t) \simeq (1-\delta_{ij})\, H_n e^{i\Psi_n} \exp\{-4\pi i \frac{r_n}{\lambda_o}[\hat{R}_A(t_o)\cdot \hat{r}_n(t_o) - (t-t_o)\hat{R}_A(t_o) \times \hat{r}_n(t_o)\cdot\vec{\Omega}(t_o)]\}, \qquad (4.13)$$

where the superscript "M" reminds us that it is for the monostatic case, the exponential has been linearized in terms of small quantities, and

$$\vec{\Omega}(t) \equiv \vec{\omega}(t) - \vec{\omega}_A(t) \quad . \qquad (4.14)$$

Similarly for the bistatic case (with superscript "B" as indicator):

$$C^{B}_{ij}(t) \simeq (1 - \delta_{ij}) H_n e^{i\Psi_n} \exp\{-4\pi i \frac{r_n}{\lambda_o} \cos(\frac{\beta}{2}) [\hat{R}_{AB}(t_o) \cdot r_n(t_o)$$

$$- (t-t_o)\hat{R}_{AB}(t_o) \times \hat{r}_n(t_o) \cdot \vec{\Omega}(t_o)]\} \qquad (4.15)$$

Suppose now that the target object is made up of N such isotropic point scatterers, and that as ideal points they never block or shadow one another. Then the total scattering matrix for the entire object is found by letting each element be the sum of N terms of the form (4.13) or (4.15). Or alternatively the total scattering matrix may be thought of as the sum of N scattering matrices, each with elements of the form (4.13) or (4.15). These two pictures are mathematically equivalent, and represent in terms of this simple scattering center model what one should expect to measure as the scattering matrix over the time interval from $t_o - \frac{T}{2}$ to $t_o + \frac{T}{2}$.

For the measured scattering matrix we attempt to resolve the individual scattering centers in "Doppler" by performing a finite Fourier Transform of the matrix elements. Let's see what this corresponds to in terms of the model. The finite Fourier Transform of a function S(t) on the interval $t_o - \frac{T}{2} \le t \le t_o + \frac{T}{2}$ is defined to be

$$\tilde{S}(f) \equiv \int_{t_o - \frac{T}{2}}^{t_o + \frac{T}{2}} S(t)\, e^{-2\pi i f(t-t_o)}\, dt \quad . \tag{4.16}$$

Operating thus on the sum of terms of the form (4.13) we find that

$$\tilde{C}^M_{ij}(f) \simeq (1-\delta_{ij})\, T \sum_{n=1}^{N} H_n e^{i\phi^A_n}\, j_o\, [\pi\, T(f-f^A_n)] \ , \tag{4.17}$$

where

$$\phi^A_n \equiv \Psi_n - 4\pi \frac{r_n}{\lambda_o} \hat{R}_A(t_o) \cdot \hat{r}_n(t_o) \ , \tag{4.18}$$

$$f^A_n \equiv \frac{2r_n}{\lambda_o} \hat{R}_A(t_o) \times \hat{r}_n(t_o) \cdot \vec{\Omega}(t_o) \, , \tag{4.19}$$

and $j_o(x)$ is the Spherical Bessel Function of order zero, given by

$$j_o(x) \equiv \frac{\sin x}{x} \equiv \text{sinc}\ (x/\pi) \quad . \tag{4.20}$$

The equivalent expression in the bistatic case is

$$\tilde{C}^{B}_{ij}(f) \simeq (1-\delta_{ij})\ T \sum_{n=1}^{N} H_n e^{i\phi^{B}_{n}}\ j_o[\pi\ T(f-f^{B}_{n})]\ , \tag{4.21}$$

where

$$\phi^{B}_{n} \equiv \Psi_n - 4\pi \frac{r_n}{\lambda_o} \hat{R}_{AB}(t_o) \cdot \hat{r}_n(t_o) \cos\left(\frac{\beta}{2}\right) \tag{4.22}$$

and

$$f^{B}_{n} \equiv 2 \frac{r_n}{\lambda_o} \hat{R}_{AB}(t_o) \times \hat{r}_n(t_o) \cdot \vec{\Omega}\ (t_o) \cos\left(\frac{\beta}{2}\right). \tag{4.23}$$

The Fourier Transformed scattering matrix elements $\tilde{C}_{ij}(f)$ correspond to the results of the "Doppler mapping" process. They will be discussed in some detail in a later section, but at the present time, we wish to comment on just one thing: the fact that each term of the sums in (4.17) and (4.21) contains a function of the form $F_n(f) \equiv TH_n j_o[\pi T(f-f_n)]$. This function has a strong main peak at $f=f_n$ and lesser subsidiary peaks in the sidelobes; the amplitude of the main peak is given by TH_n and its width is proportional to $(\pi\ T)^{-1}$. This behavior is the explanation for the fact that the modulus of the "Doppler maps" contains sharp peaks at values of the frequency corresponding to individual resolved scattering centers.

A bit of further realism can be added to this model if we allow for the possibility of shadowing. In a real object, made up of non-ideal scatterers, there is a good chance that during the time of integration $|t-t_o| \leq \frac{T}{2}$ some of the scattering centers will not be seen at all (being "in shadow" the whole time) and others will be seen only part of the time (entering or emerging from the shadow at some points in the integration interval). The completely shadowed point is easy to treat: it simply makes no contribution at all to the scattering matrix. What about the other case? Suppose a point "ℓ" is visible from $t=t_o - t_1$ until $t=t_o + t_2$, where $-\frac{T}{2} \leq -t_1 < t_2 \leq \frac{T}{2}$, and is invisible during the rest of the interval. In this case a straightforward integration shows that the transformed scattering matrix has the form

$$\tilde{C}_{ij}(f) \simeq (1-\delta_{ij})\ \chi_\ell\ TH_\ell e^{i\phi_\ell} \exp[-i\pi(t_2-t_1)(f-f_\ell)]\, j_o[\pi\chi_\ell\ T(f-f_\ell)], \qquad (4.24)$$

where $\chi_\ell \equiv (t_1+t_2)/T$ represents the fraction of the total integration interval for which the scatterer is visible, and where $\phi_\ell \equiv \phi_\ell^A$ or ϕ_ℓ^B and $f_\ell \equiv f_\ell^A$ or f_ℓ^B depending on whether the situation is monostatic or bistatic.

Clearly, then, the effect of the partial shadowing is (a) to decrease the amplitude and increase the width of the corresponding peak of the Doppler map modulus in proportion to the fraction of the integration time spent in shadow, and (b) to insert a phase change proportional to $(t_2-t_1)(f-f_\ell)$, so that there is no phase change if the visible "window" is evenly centered

in the integration interval, and in any case there is no phase change at $f=f_\ell$: the center of the peak.

Further comments concerning these scattering matrix elements will be reserved for a later section.

SECTION V

FIXED POINT DIPOLE SCATTERERS

The simplest model of a scattering center which depolarizes and has "orientability" is the fixed point dipole, by which we mean a point dipole of dipole moment $\vec{p}_n(t)$ rigidly connected, by a vector $\vec{r}_n(t)$, to the object's center of mass, 0, and rigidly rotating about 0 with the object's angular velocity $\vec{\omega}(t)$. The magnitudes r_n and p_n are constant, independent of t. When we say that the vector $\vec{p}_n$ is rigidly connected by $\vec{r}_n$ to 0, we mean that $\vec{p}_n$ transforms in the same way as $\vec{r}_n$ under rotation about 0, i.e.

$$\frac{d}{dt}\vec{p}_n \equiv \vec{\omega}(t) \times \vec{p}_n(t). \tag{5.1}$$

This may either be regarded as a definition of "fixed point dipole", or may be shown to follow necessarily from a mathematical formulation of what one might intuitively mean by the statement that $\vec{p}_n$ is "rigidly" connected by $\vec{r}_n$ to 0: See Appendix B.

Suppose now that a unit signal with linear polarization $\hat{E}_T \equiv \hat{e}_j$ is transmitted by antenna A toward the target. The excitation of dipole n by this signal will be proportional to $\hat{E}_T \cdot \hat{p}_n$. The dipole then begins to radiate, and the appropriate formula for the far-field radiation of an oscillating electric dipole tells us that as it approaches the receivers the reradiated signal is proportional to the excitation and to

$$\hat{R}_A \times (\vec{p}_n \times \hat{R}_A) \qquad \text{in the monostatic case}$$

and to

$$\hat{R}_B \times (\vec{p}_n \times R_B) \qquad \text{in the bistatic case.}$$

Therefore, in the notation of Section III,

$$\sigma\hat{E}_T \equiv (\hat{e}_j \cdot \hat{p}_n)[\hat{R}_A \times (\vec{p}_n \times \hat{R}_A)] \tag{5.2a}$$

and

$$\sigma'\hat{E}_T \equiv (\hat{e}_j \cdot \hat{p}_n)[\hat{R}_B \times (\vec{p}_n \times \hat{R}_B)] \tag{5.2b}$$

If the receiving antenna has linear polarization given by

(monostatic): $$\hat{E}_R^A \equiv \hat{e}_i$$

(bistatic) : $$\hat{E}_R^B \equiv \hat{e}_i' \quad , \tag{5.3}$$

and we recall that $\hat{e}_i \cdot \hat{R}_A \equiv 0$ and $\hat{e}_i' \cdot \hat{R}_B \equiv 0$, then the received signal is characterized by

(monostatic): $$\hat{E}_R^A \cdot \sigma\hat{E}_T = p_n(\hat{e}_j \cdot \hat{p}_n)(\hat{e}_i \cdot \hat{p}_n) \tag{5.4a}$$

(bistatic) : $$\hat{E}_R^B \cdot \sigma'\hat{E}_T = p_n(\hat{e}_j \cdot \hat{p}_n)(\hat{e}_i' \cdot \hat{p}_n) \; . \tag{5.4b}$$

Making use now of eq. (3.5), the comment at the end of Section III, and the definition of Scattering Matrix, we see that in the linear basis and for the monostatic case the scattering matrix for the n^{th} dipole has the elements

$$S^M_{ij} = p_n(\hat{e}_i \cdot \hat{p}_n)(\hat{e}_j \cdot \hat{p}_n) \exp[-4\pi i \frac{r_n}{\lambda_o} \hat{R}_A \cdot \hat{r}_n]. \qquad (5.5)$$

For the bistatic case the scattering matrix elements are

$$S^B_{ij} = p_n(\hat{e}'_i \cdot \hat{p}_n)(\hat{e}_j \cdot \hat{p}_n) \exp[-4\pi i \frac{r_n}{\lambda_o} \hat{R}_{AB} \cdot \hat{r}_n \cos(\frac{\beta}{2})]. \qquad (5.6)$$

Notice that, as required, $\lim_{\beta \to 0} S^B_{ij} = S^M_{ij}$, since $\hat{e}'_i \to \hat{e}_i$ and $\hat{R}_{AB} \to \hat{R}_A$ as $\beta \to 0$.

Now we must make the transformation into the circular basis. We define

$$\xi^M_n \equiv 4\pi \frac{r_n}{\lambda_o} \hat{R}_A \cdot \hat{r}_n \qquad (5.7)$$

and use eqns (2.14) to find the scattering matrix elements in the monostatic case:

$$C_{11}^M = \tfrac{1}{2}p_n e^{-i\xi_n^M}\left[(\hat{e}_1\cdot\hat{p}_n)^2 - (\hat{e}_2\cdot\hat{p}_n)^2 + 2i(\hat{e}_1\cdot\hat{p}_n)(\hat{e}_2\cdot\hat{p}_n)\right] \qquad (5.8a)$$

$$C_{12}^M \equiv C_{21}^M = \tfrac{1}{2}p_n e^{-i\xi_n^M}\left[(\hat{e}_1\cdot\hat{p}_n)^2 + (\hat{e}_2\cdot\hat{p}_n)^2\right] \qquad (5.8b)$$

$$C_{22}^M = \tfrac{1}{2}p_n e^{-i\xi_n^M}\left[(\hat{e}_1\cdot\hat{p}_n)^2 - (\hat{e}_2\cdot\hat{p}_n)^2 - 2i(\hat{e}_1\cdot\hat{p}_n)(\hat{e}_2\cdot\hat{p}_n)\right]. \qquad (5.8c)$$

The bistatic case is somewhat more complicated: because of the presence of the primes in eq. (5.6) the expressions found upon using eqns. (2.16) do not simplify very much since, for example, $S_{12}^B \neq S_{21}^B$. But for small bistatic angles these difficulties can be removed. Suppose we define basis vectors $\hat{e}_i''$ in a plane normal to $\hat{R}_{AB}$ in analogy to the definitions of $\hat{e}_i$ in a plane normal to $\hat{R}_A$. Then it can be shown [see Appendix A] that to order $O(\frac{\beta}{2})^2$ the elements of the scattering matrix in the circular basis and the bistatic case can be found from those in the monostatic case by simply replacing $\hat{e}_i$ by $\hat{e}_i''$ and ξ_n^M by ξ_n^B, where

$$\xi_n^B = 4\pi\frac{r_n}{\lambda_o}\,\hat{R}_{AB}\cdot\hat{r}_n\cos(\tfrac{\beta}{2}) \,. \qquad (5.9)$$

This statement may be considered to be the form of the monostatic-bistatic equivalence theorem for a point dipole scatterer. It should be carefully

noted that this equivalence does not hold true for the scattering matrix in the linear basis.

Hereafter we shall consider only the monostatic case, the bistatic one being deriveable from it by the above transformations.

The scattering matrix elements can be expressed in a simple way in terms of meaningful geometrical quantities. The plane defined by $\hat{e}_1$ and $\hat{e}_2$ is often called the radar polarization plane. The projection of the vector $\hat{p}_n$ onto this plane makes an angle θ_n with the $\hat{e}_1$-axis, and this angle is often called the Polarization Angle of the dipole. Similarly, the projection of $\hat{p}_n$ onto the vector $\hat{R}_A$ (normal to the Polarization Plane) defines the Aspect Angle, ζ_n, of the dipole. See Figure 3 below:

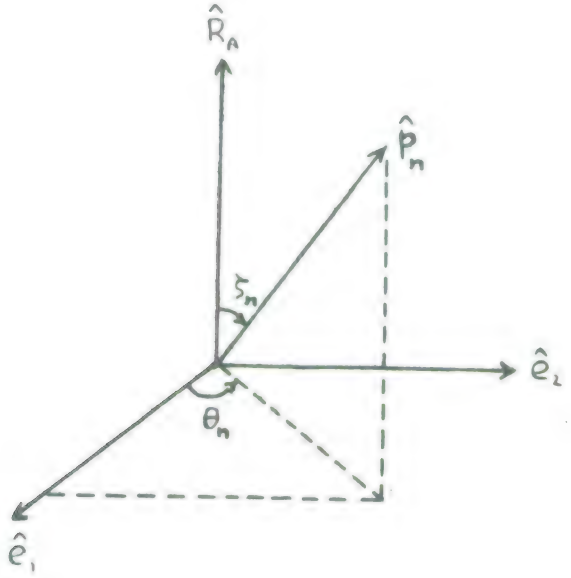

Figure 3. Decomposition of the Vector $\hat{p}_n$.

Notice that

$$\hat{R}_A \cdot \hat{p}_n \equiv \cos \zeta_n$$

$$\hat{e}_1 \cdot \hat{p}_n \equiv \sin \zeta_n \cos \theta_n$$

$$\hat{e}_2 \cdot \hat{p}_n \equiv \sin \zeta_n \sin \theta_n \qquad (5.10)$$

If we substitute eqns (5.10) into (5.8) we easily find the scattering matrix elements

$$C_{11} = \tfrac{1}{2} p_n \sin^2 \zeta_n e^{-(\xi_n - 2\theta_n)}$$

$$C_{12} = C_{21} = \tfrac{1}{2} p_n \sin^2 \zeta_n \, e^{-i\xi_n}$$

$$C_{22} = \tfrac{1}{2} p_n \sin^2 \zeta_n e^{-i(\xi_n + 2\theta_n)} \; . \qquad (5.11)$$

These can all be stated in one equation:

$$C_{ij} = \tfrac{1}{2} p_n \sin^2 \zeta_n \exp\{-i[\xi_n + 2\delta_{ij}(-1)^j \theta_n]\} \; . \qquad (5.12)$$

The next step is to find the time dependence of these matrix elements. Now, the time dependence of ξ_n has already been discussed in Section IV [see eqns (4.13) and (4.15)]. The factor $\sin^2\zeta_n(t)$ can be expanded in Taylor series, making use of eqns (5.10), (4.10), and (5.1) along the way, and linearized in terms of small quantities as has been done before; the result is

$$\sin^2\zeta_n(t) \simeq \sin^2\zeta_n(t_o) + 2(t-t_o)\cos\zeta_n(t_o)\,\hat{R}_A(t_o) \times \hat{p}_n(t_o)\cdot\vec{\Omega}(t_o). \quad (5.13)$$

and finally we may write for $\theta_n(t)$ the expression

$$\theta_n(t) \simeq \theta_n(t_o) + (t-t_o)\,\dot{\theta}_n(t_o). \quad (5.14)$$

That the linearization here is legitimate may be shown by expressing $\dot{\theta}_n$ in terms of more fundamental quantities; it turns out to be of first order in small quantities like $\vec{\omega}$ and $\vec{\omega}_A$, with higher derivitives being of higher order. The complete expression for $\dot{\theta}_n$ is not simple, but it may be important in later stages of analysis to know its form, so it is derived and discussed in Appendix C.

Now the linearized time dependence of C_{ij} can be written down.

Let

$$f_n \equiv 2 \frac{r_n}{\lambda_o} \hat{R}_A(t_o) \times \hat{r}_n(t_o) \cdot \vec{\Omega}(t_o), \tag{5.15}$$

$$g_n \Omega(t_o) \sin \zeta_n(t_o) \equiv \hat{R}_A(t_o) \times \hat{p}_n(t_o) \cdot \vec{\Omega}(t_o), \tag{5.16}$$

and

$$\phi_n \equiv 4\pi \frac{r_n}{\lambda_o} \hat{R}_A(t_o) \cdot \hat{r}_n(t_o) \cos \left(\frac{\beta}{2}\right) \tag{5.17}$$

where $\hat{R}_A \leftarrow \hat{R}_{AB}$ in the bistatic case

and $\beta \equiv 0$ in the monostatic case.

Then

$$C_{ij}(t) \simeq \tfrac{1}{2} p_n \sin \zeta_n(t_o) [\sin \zeta_n(t_o) + 2(t-t_o) g_n \Omega(t_o) \cos \zeta_n(t_o)]$$

$$\exp\{-i[\phi_n + 2\delta_{ij}(-1)^j \theta_n(t_o)]\} \exp\{2\pi i (t-t_o)[f_n - \frac{1}{\pi} \delta_{ij}(-1)^j \dot{\theta}_n(t_o)]\} . \tag{5.18}$$

Suppose now that the target is made up of M such point dipole scatterers, and that as ideal points they never block or shadow one another. Then the total scattering matrix for the entire object is found by letting each element be the sum of M terms of the form (5.18). In terms of our simple scattering center model this represents what one should expect to measure

as the scattering matrix over the time interval $|t-t_o| \leq \frac{T}{2}$.

Applying the finite Fourier transform (4.16) to this sum of terms we find that

$$\tilde{C}_{ij}(f) \simeq \sum_{m=1}^{M} G_m(f)\, e^{-i\phi_m^*} \tag{5.19}$$

where

$$G_m(f) \equiv \tfrac{1}{2} T p_m \sin\zeta_m(t_o) \{\sin\zeta_m(t_o)\, j_o[\pi T(f-f_m^*)]$$

$$- iTg_m\Omega(t_o)\cos\zeta_m(t_o) j_1[\pi T(f-f_m^*)]\}, \tag{5.20}$$

with

$$\phi_m^* \equiv \phi_m + 2\delta_{ij}(-1)^j\, \theta_m(t_o), \tag{5.21}$$

$$f_m^* \equiv f_m - \frac{1}{\pi}\,\delta_{ij}(-1)^j\, \dot{\theta}_m(t_o), \tag{5.22}$$

and $j_1(x)$ is the Spherical Bessel Function of order one, given by

$$j_1(x) \equiv \frac{1}{x}\left(\frac{\sin x}{x} - \cos x\right). \tag{5.23}$$

These Fourier-Transformed scattering matrix elements $\tilde{C}_{ij}(f)$ should correspond to the results of the Doppler mapping process. They will be discussed in some detail in a later section, but at the present time we

wish merely to point out that the modulus of $G_m(f)$ usually has a peak at $f=f_m^*$, though both the magnitude and the width of this peak vary strongly with the aspect angle $\zeta_m(t_o)$ and for sufficiently small values of ζ_m it may be so small and broad as to escape notice. The rather complicated function $G_m(f)$ will be examined more fully later.

Notice that when a recognizable peak does occur at $f=f_m^*$ for a particular scatterer, it does not appear in the same place in each of the four Doppler maps. Its location will be the same for the two off-diagonal elements, and it will appear in the diagonal elements shifted by equal amounts in opposite directions. This shift may make the process of associating corresponding peaks more difficult, but on the other hand if the association can be made then the shift provides useful information about the dipole involved:

$$\Delta f_m \equiv f_{22} - f_{11} = \frac{2}{\pi} \dot{\theta}_m(t_o).$$

Similarly the shift in the phases corresponding to these two diagonal peaks, if it can be determined, yields the polarization angle directly:

$$\Delta\phi_m \equiv \phi_{22} - \phi_{11} = -4\theta_m(t_o) .$$

As in the case of isotropic point scatterers, further realism can be added to the model by allowing for the possibility of shadowing. Once again, as at the end of Section IV, we consider a scattering center "ℓ" which is visible from $t=t_o - t_1$ till $t=t_o + t_2$, where $-\frac{T}{2} \le -t_1 < t_2 \le \frac{T}{2}$

and $t_1 + t_2 \equiv \chi_\ell T$. Then the transformed scattering matrix for this scatterer takes the form

$$\tilde{C}_{ij}(f) \simeq \tfrac{1}{2}\chi_\ell T p_\ell \sin\zeta_\ell(t_o) e^{-i\phi^*_\ell} \exp[-i\pi(t_2 - t_1)(f-f^*_\ell)] \{[\sin\zeta_\ell(t_o)$$

$$+ (t_2 - t_1)\, g_\ell\, \Omega(t_o) \cos\zeta_\ell(t_o)]\, j_o[\pi\chi_\ell T(f-f^*_\ell)]$$

$$- i\chi_\ell T g_\ell\, \Omega(t_o) \cos\zeta_\ell(t_o)\, j_1[\pi\chi_\ell T(f-f^*_\ell)]\} \,. \qquad (5.24)$$

The same comments which were made (at the end of Section IV) about the results of shadowing for isotropic point scatterers, Eq. (4.24), also hold true about the above results of shadowing for point dipole scatterers. The modulus peaks are reduced in magnitude and increased in width, and a phase term is inserted which vanishes when $f=f^*_\ell$ and which is proportional to the "asymmetry of the shadowing": $t_2 - t_1$.

SECTION VI

SOME REMARKS CONCERNING THE DOPPLER MAP FUNCTIONS

Consider now a complex target composed of N scatterers, some being isotropic points as described in Section IV and the others being point dipoles as described in Section V. The transformed scattering matrix or "Doppler Map Function" for this target may be written in the form

$$\tilde{C}_{ij}(f) \simeq \sum_{n=1}^{N} M_n(ij,f) \quad \exp\left\{ iA_n(ij, f) \right\} \tag{6.1}$$

where the functions M_n and A_n depend in form on whether scatterer n is an isotropic point or a point dipole, and where the bistatic cases are referred back to the appropriate monostatic situations by invoking the monostatic-bistatic equivalence theorem. Allowing for the effects of shadowing, these functions are:

(1) for isotropic point scatterers, using eq. (4.24):

$$M_n(ij,f) = (1-\delta_{ij})\, \chi_n\, TH_n\, j_o\left[\pi\chi_n T(f-f_n)\right] \tag{6.2}$$

$$A_n(ij,f) = \phi_n - \pi(t_2-t_1)(f-f_n), \tag{6.3}$$

with

$$f_n = \frac{2r_n}{\lambda_o}\, \hat{R}_A(t_o) \times \hat{r}_n(t_o) \cdot \vec{\Omega}(t_o), \tag{6.4}$$

$$\phi_n = \psi_n - 4\pi \frac{r_n}{\lambda_o} \hat{R}_A(t_o) \cdot \hat{r}_n(t_o) \cos(\frac{\beta}{2}), \tag{6.5}$$

where $\hat{R}_A \leftarrow \hat{R}_{AB}$ in the bistatic case and $\beta \equiv 0$ in the monostatic case;

(2) for point dipole scatterers, using eq. (5.24):

$$M_n(ij,f) = \tfrac{1}{2} \chi_n T p_n \sin \zeta_n(t_o) \; |G_n(ij,f)| \tag{6.6}$$

$$A_n(ij,f) = \phi_n^*(ij) - \pi(t_2-t_1)[f-f_n^*(ij)] + \gamma_n(ij,f), \tag{6.7}$$

$$|G_n(ij,f)|^2 \equiv [\sin \zeta_n(t_o) + (t_2-t_1)\, g_n \Omega(t_o) \cos \zeta_n(t_o)]\{j_o[\pi\chi_n T(f-f_n^*(ij))]\}^2$$

$$+ [\chi_n T g_n \, \Omega(t_o) \cos \zeta_n(t_o)]^2 \{j_1[\pi\chi_n T(f-f_n^*(ij))]\}^2, \tag{6.8}$$

$$\tan \gamma_n(ij,f) \equiv \frac{\chi_n T g_n \, \Omega(t_o) \cos \zeta_n(t_o)}{\sin \zeta_n(t_o) + (t_2-t_1) g_n \Omega(t_o) \cos \zeta_n(t_o)} \; \frac{j_1[\pi\chi_n T(f-f_n^*(ij))]}{j_o[\pi\chi_n T(f-f_n^*(ij))]}, \tag{6.9}$$

$$f_n^*(ij) \equiv f_n - \frac{1}{\pi} \delta_{ij}(-1)^j \dot{\theta}_n(t_o), \tag{6.10}$$

$$\phi^{*}_{n}(ij) \equiv -4\pi \frac{r_n}{\lambda_o} \hat{R}_A(t_o) \cdot \hat{r}_n(t_o) \cos(\tfrac{\beta}{2}) - 2\delta_{ij}(-1)^j \theta_n(t_o), \qquad (6.11)$$

where

$$g_n \Omega(t_o) \sin \zeta_n(t_o) \equiv \hat{R}_A(t_o) \times \hat{p}_n(t_o) \cdot \vec{\Omega}(t_o), \qquad (6.12)$$

$\hat{R}_A \leftarrow \hat{R}_{AB}$ in the bistatic case,

and

$\beta \equiv 0$ in the monostatic case.

Equation (6.12) defines the quantity g_n, whose absolute value is less than unity.

It has been found most convenient to display experimentally-determined "Doppler Maps" in the form of modulus and argument of the complex function plotted against frequency f. So for comparison with experiment we express eq. (6.1) in the form

$$\tilde{C}_{ij}(f) \simeq M_{ij}(f) \exp\{iA_{ij}(f)\}, \qquad (6.13)$$

where it is not difficult to see that

$$M^2_{ij}(f) = \sum_{n=1}^{N}\sum_{m=1}^{N} M_n(ij,f)\, M_m(ij,f) \cos[A_n(ij,f) - A_m(ij,f)], \qquad (6.14)$$

and

$$\tan A_{ij}(f) = \frac{\sum_{n=1}^{N} M_n(ij,f) \sin A_n(ij,f)}{\sum_{n=1}^{N} M_n(ij,f) \cos A_n(ij,f)} \qquad (6.15)$$

The behavior of $M_{ij}(f)$ and $A_{ij}(f)$ as functions of f depend primarily on the form of the functions $M_n(ij,f)$. Qualitatively, as has already been remarked, these functions usually (though not always: see below) are more or less sharply peaked at $f=f_n$ and relatively small elsewhere; i.e., they are rough approximations to $\delta(f-f_n)$. Even if for certain types of scattering centers the functions $M_n(ij,f)$ do not have the precise forms shown in Equations (6.2) or (6.6), it is reasonable to assume that in most cases they will have the same qualitative properties, so that the argument below is still applicable.

Now if $M_n(ij,f)$ were indeed very close to a true delta function (which would be the ideal situation), what should we expect to happen? Well, equations (6.14) and (6.15) would then be effectively "decoupled", in the sense that we would have

$$M_{ij}(f) = \begin{cases} M_n(ij,f_n) \text{ at } f=f_n \text{ for any } n \\ \\ \sim 0 \text{ at } f \neq f_n \text{ for any } n \end{cases}$$

$$A_{ij}(f) = \begin{cases} A_n(ij,f_n) \text{ at } f=f_n \text{ for any } n \\ \\ \text{random} \quad \text{at } f \neq f_n \text{ for any } n \end{cases} .$$

Thereupon by observing the locations of the peaks in the modulus of the Doppler Map function we could easily find the true values of f_n and ϕ_n (mod 2π) and be well on the way towards solving for the locations, motions, and orientations (if applicable) of all the scatterers. [If scatterer n is a dipole, substitute f_n^* and ϕ_n^* for f_n and ϕ_n everywhere in this paragraph.]

But if $M_n(ij,f)$ is not very close to a perfect delta function, but rather has significant sidelobes, then the different terms of equations (6.14) and (6.15) become seriously cross-coupled. This inter-modulation, as it may be called, has three deleterious effects, all of which have been easily observed in simulated data made up to satisfy Eq. (6.2). These are:

1. Spurious peaks may appear in the modulus function at values of f not corresponding to any true scatterer.

2. The values of f at which genuine peaks appear in the modulus function are somewhat displaced from the correct values f_n or f_n^*

3. The values of the argument corresponding to peaks in the modulus function are somewhat displaced from the correct values ϕ_n or ϕ_n^*.

These problems can, if sufficiently severe, make correct interpretation of the data rather difficult. Therefore it is important to try to ensure that the functions $M_n(ij,f)$ are reasonably good approximations to delta functions. Naturally, we can't change the data as the target presents them to us. But it may be possible to take steps during the Fourier integration procedure to enable the functions M_n to have peaks as narrow and sidelobes as low as the natures of the individual scattering centers allow. Amplitude weighting, for example, can considerably reduce the sidelobes, although at the cost of some broadening of the peaks. Increasing the integration time T with the help of previously estimated body motion constraints might go a long way toward alleviating this problem, if it can be done.

After the above discussion involving the general porperties of the functions $M_n(ij,f)$, this seems a good place to illustrate the specific forms of the moduli $|M_n|$ for certain typical cases.

First of all, for isotropic point scatterers Eq. (6.2) shows that $|M_n(ij,f)| \equiv 0$ for $ij=11$ or 22, and that $|M_n(ij,f)| = T\chi_n H_n |j_o[\pi T\chi_n(f-f_n)]|$ for $ij = 12$ or 21. Figure 4 shows a graph of $|j_o(x)|$ and $|j_1(x)|$: it is easy to see that the maximum value of $|M_n|$ is given by $T\chi_n H_n$ and occurs at $f=f_n$. The first sidelobe maximum occurs at $f \simeq f_n \pm \frac{4.50}{\pi T\chi_n}$, and its value is approximately given by $0.22\, T\chi_n H_n$, down only 6.6 db from the peak. The 3 db width of the main peak is $\Delta f = 3.8/\pi T\chi_n$. Of course appropriate weighting reduces the sidelobe level considerably whilst increasing the width of the peak, so there isn't really much

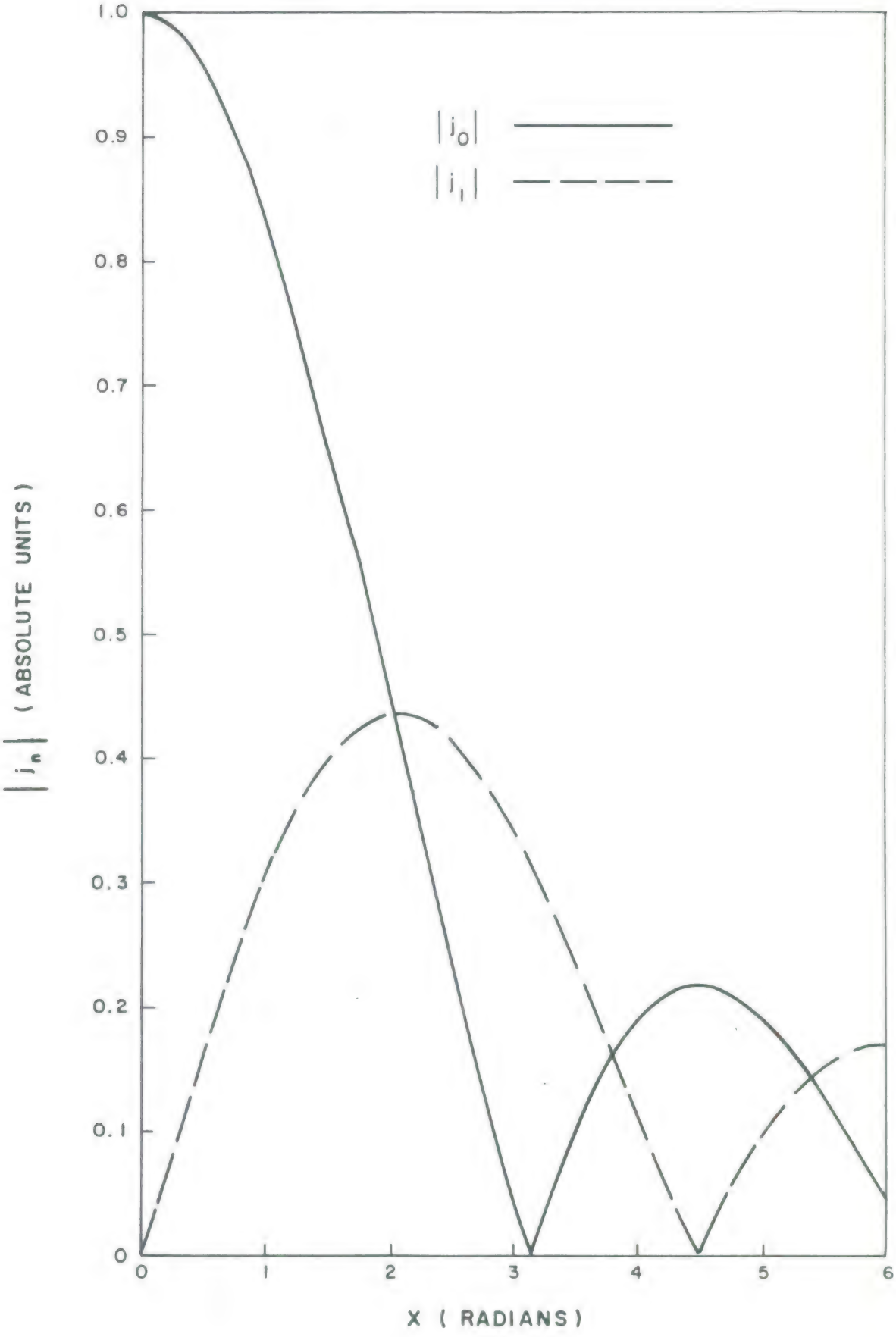

IB- 25,454

Figure 4. ABSOLUTE VALUES OF THE FIRST TWO SPHERICAL BESSEL FUNCTIONS

point in using the exact values just quoted above except as indications of how the moduli $|M_n|$ behave as functions of the parameters T, χ_n and H_n.

For point dipole scatterers the situation is considerably more complicated and is made even more so when weighting is used. To get at least some feel for the behavior of $|M_n(ij,f)|$ under several different sets of parameters, consider Figures 5 through 9. The functions plotted here are

$$|M(x)| \equiv |\sin \zeta| [\sin^2 \zeta j_o^2(x) + \epsilon^2 \cos^2 \zeta j_1^2(x)]^{\frac{1}{2}} \qquad (6.16)$$

for various values of the parameters ζ and ϵ, using the same relative scale of units for all five graphs. Referring to Eqns.(6.6) and (6.8), it is clear that these functions represent $|M_n|$ for fixed values of p_n, T, and χ_n, plotted against the independent variable

$$x \equiv \pi \chi_n T(f-f_n^*),$$

with $t_1 \equiv t_2$ and $\epsilon \equiv \chi_n T g_n \Omega$. Under ordinary conditions the parameter ϵ will have absolute value less than unity, so this is the range of values used in Figures 5-9; the values of aspect angle ζ used in the figures are a representative sample: 10^o, 30^o, 45^o, 60^o, and 80^o. Based on these figures several observations should be made.

(1) Except for the smallest aspect angles, the functions all behave qualitatively like $|j_o(x)|$ in that they have a main peak at x=0

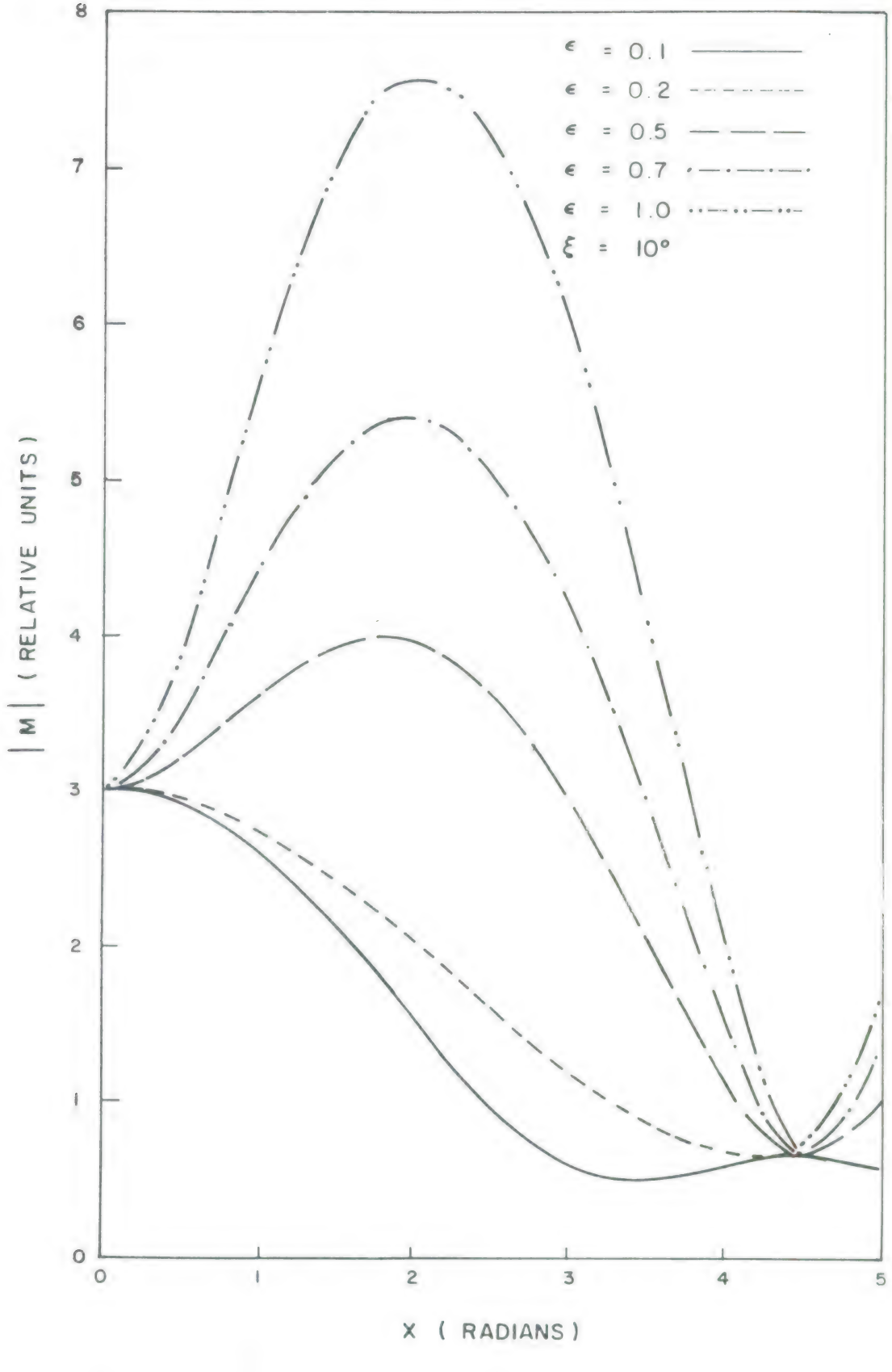

IA-25,457

Figure 5. THE FUNCTION $|M(X)|$ FOR $\xi = 10°$ AND VARIOUS VALUES OF ϵ

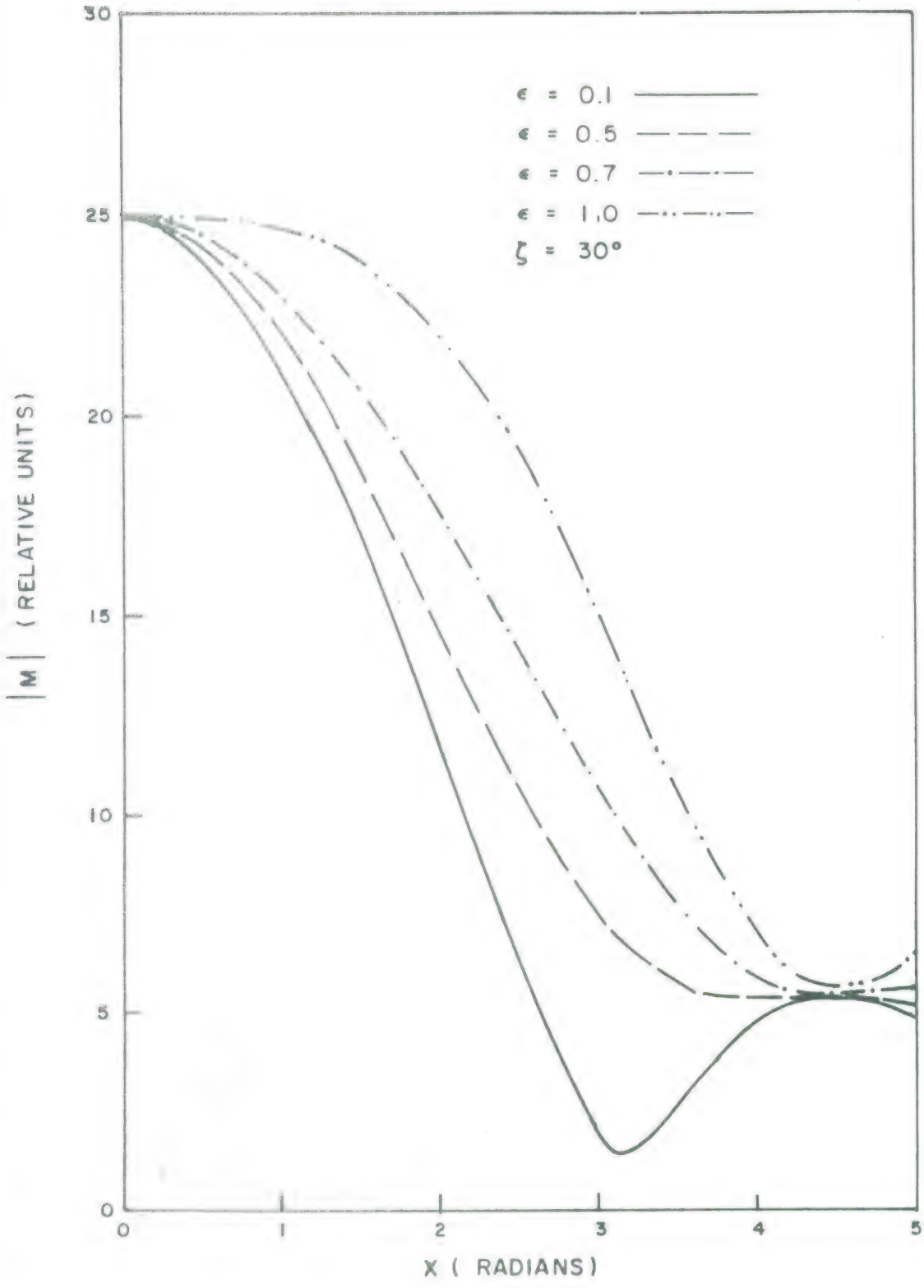

IA-25,455

Figure 6. THE FUNCTION |M(X)| FOR $\zeta = 30°$ AND VARIOUS VALUES OF ϵ

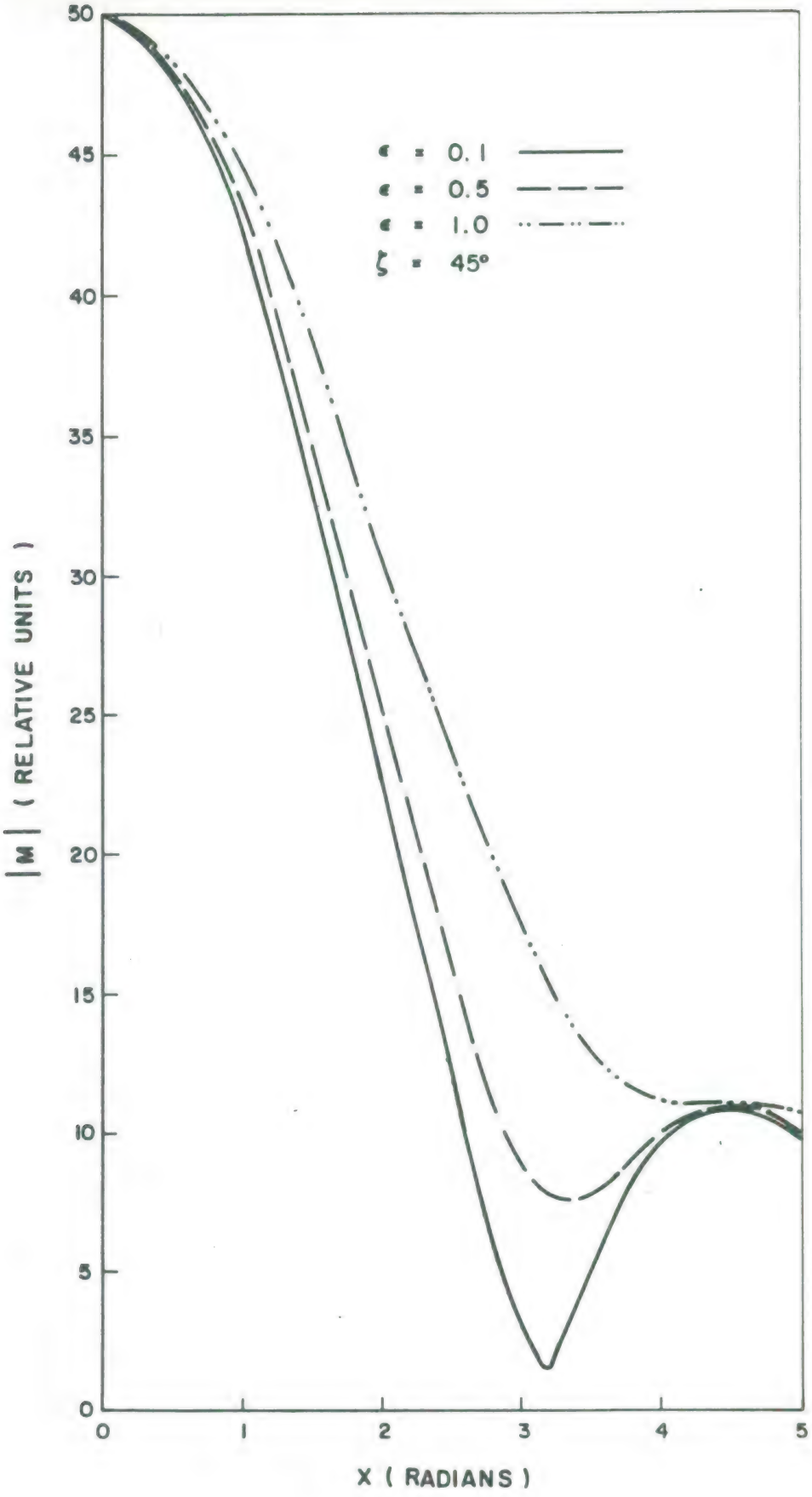

18 – 25,452

Figure 7. THE FUNCTION $|M(X)|$ FOR $\zeta = 45°$ AND VARIOUS VALUES OF ϵ

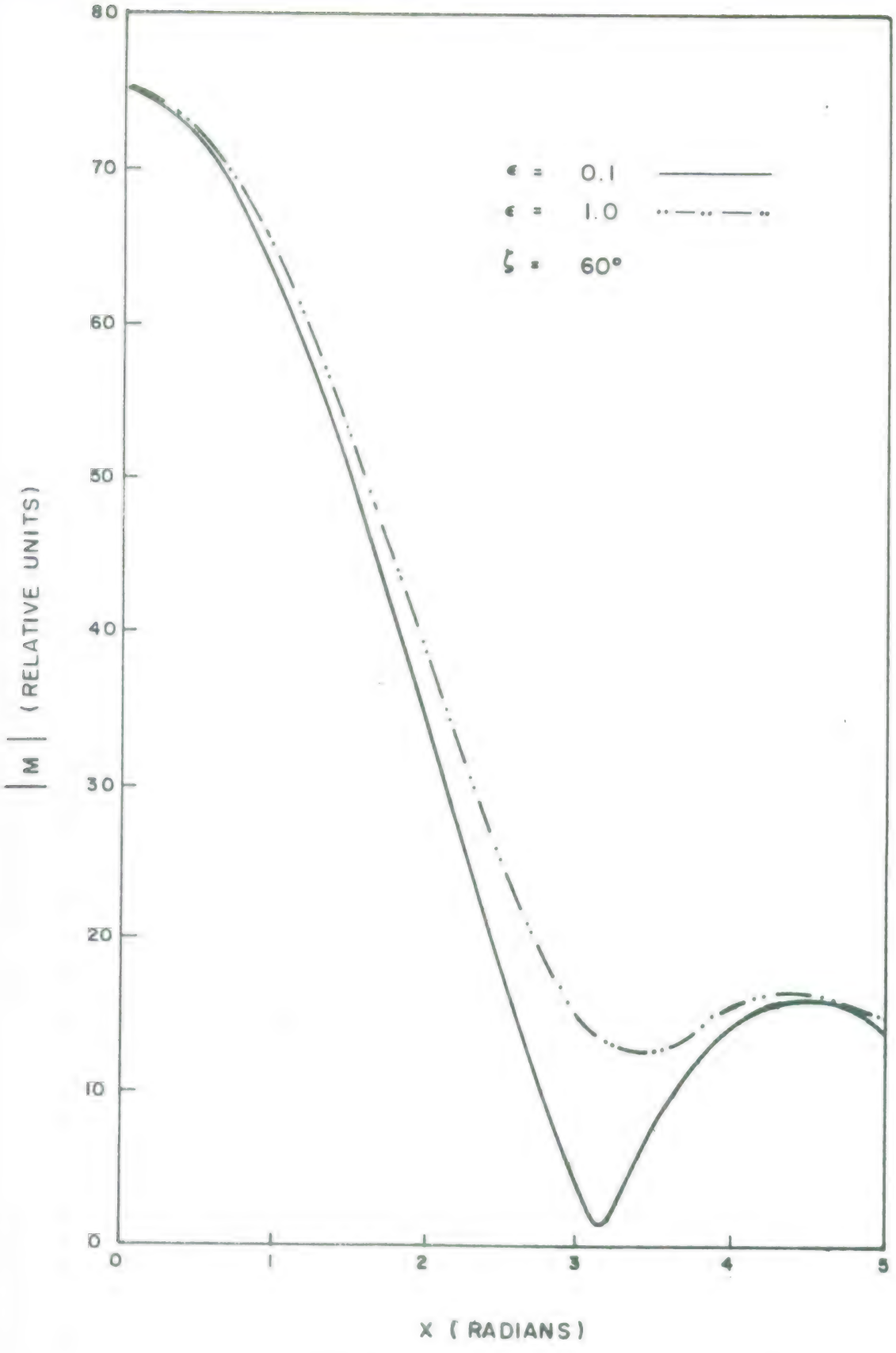

IA-25,456

Figure 8. THE FUNCTION $|M(X)|$ FOR $\zeta = 60°$ AND VARIOUS VALUES OF ϵ

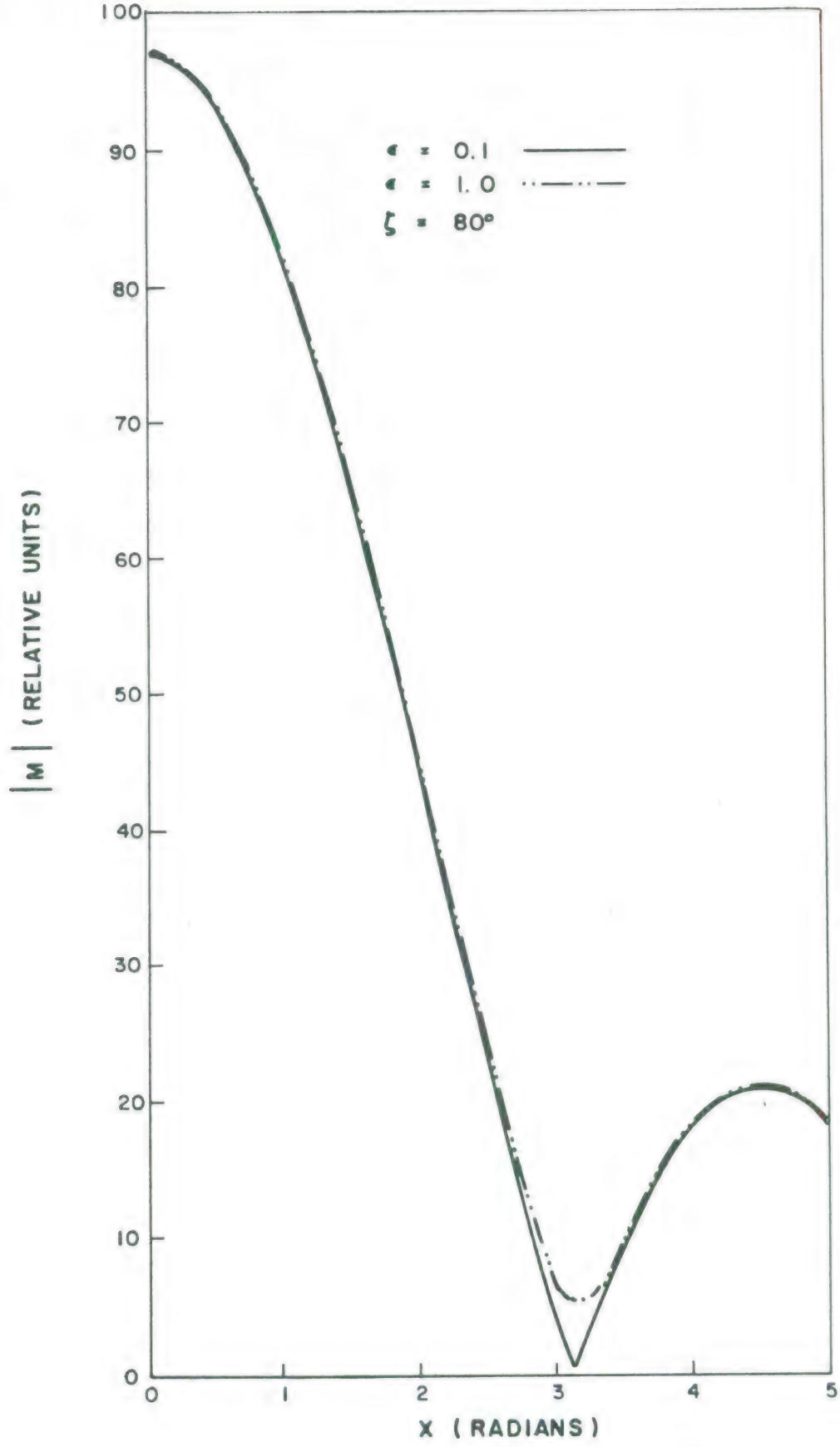

IB-25,453

Figure 9. THE FUNCTION $|M(X)|$ FOR $\zeta = 80°$ AND VARIOUS VALUES OF ϵ

and smaller sidelobe peaks at or beyond x=4.5. For small aspect angles (e.g. $\zeta = 10^{\circ}$) the main peak may, if ϵ is large enough, occur at a value of x greater than 0.

(2) The maximum value of the main peak increases rapidly with increasing aspect angle ζ. Therefore in practice the anomalistic peaks which for small ζ occur at $x \geq 0$ will not be very observable in comparison with the much larger and more "normal" peaks representing dipoles with larger values of ζ.

(3) For a given value of aspect angle ζ the width of the main peak increases with increasing ϵ, but the difference becomes smaller as ζ becomes larger, so that when $\zeta = 80^{\circ}$ the function $|M|$ is almost independent of ϵ.

APPENDIX A

THE MONOSTATIC-BISTATIC EQUIVALENCE THEOREMS

Referring back to Figure 1, we begin by defining two new unit vectors, $\hat{S}$ and $\hat{t}$:

$$\hat{S} \equiv \frac{\hat{k} + \hat{k}'}{|\hat{k} + \hat{k}'|}$$

$$\hat{t} \equiv \frac{\hat{k} - \hat{k}'}{|\hat{k} - \hat{k}'|} \quad , \tag{A-1}$$

from which it is not hard to see that

$$\hat{k} + \hat{k}' \equiv 2\hat{S} \cos\left(\frac{\beta}{2}\right)$$

and

$$\hat{k} - \hat{k}' \equiv 2\hat{t} \sin\left(\frac{\beta}{2}\right) \quad . \tag{A-2}$$

Notice that $\hat{S}$ is a unit vector in the direction of the bisector of the bistatic angle, equivalent to $\hat{R}_{AB}$ of Eq.(3.6) and others, and $\hat{t}$ is a unit vector normal to $\hat{S}$. The line-of-sight vectors $\hat{k}$ and $\hat{k}'$ can be expressed in terms of $\hat{S}$ and $\hat{t}$:

$$\hat{k} \equiv \hat{S} \cos\left(\frac{\beta}{2}\right) + \hat{t} \sin\left(\frac{\beta}{2}\right)$$

$$\hat{k}' \equiv \hat{S} \cos\left(\frac{\beta}{2}\right) - \hat{t} \sin\left(\frac{\beta}{2}\right) \quad . \tag{A-3}$$

We shall also assume that the bistatic angle is "small," meaning that we can neglect all but the lowest powers of $\beta/2$, and that $\hat{n} = \hat{n}'$ to sufficient accuracy.

Now after a great deal of inelegant and messy vector manipulations, starting with the definitions of e_i and e_i', it turns out to be possible to write

$$\begin{aligned}
\hat{e}_1 &= \hat{e}_1'' + \vec{U}\,\frac{\beta}{2} + O\left(\frac{\beta}{2}\right)^2 \\
\hat{e}_1' &= \hat{e}_1'' - \vec{U}\,\frac{\beta}{2} + O\left(\frac{\beta}{2}\right)^2 \\
\hat{e}_2 &= \hat{e}_2'' + \vec{V}\,\frac{\beta}{2} + O\left(\frac{\beta}{2}\right)^2 \\
\hat{e}_2' &= \hat{e}_2'' - \vec{V}\,\frac{\beta}{2} + O\left(\frac{\beta}{2}\right)^2 \quad ,
\end{aligned} \tag{A-4}$$

where the vectors $\hat{e}_i''$ are defined relative to $\hat{S}$ in complete analogy to the definitions of $\hat{e}_i$ relative to $\hat{k}$, and where

$$\begin{aligned}
\vec{U} &\equiv \frac{\hat{n}\cdot\hat{t}}{|\hat{n}\times\hat{S}|} + \frac{(\hat{n}\cdot\hat{S})(\hat{n}\cdot\hat{t})}{|\hat{n}\times\hat{S}|^2}\,\hat{e}_1'' \\
\vec{V} &\equiv \hat{t}\times\hat{e}_1'' - \frac{(\hat{n}\cdot\hat{S})}{|\hat{n}\times\hat{S}|^2}\,\hat{t} + \frac{(\hat{n}\cdot\hat{S})(\hat{n}\cdot\hat{t})}{|\hat{n}\times\hat{S}|^2}\,\hat{e}_2'' \quad .
\end{aligned} \tag{A-5}$$

From this result, it is obvious that

$$\hat{e}'_i \cdot \hat{e}_j \simeq \delta_{ij} - \left(\frac{\beta}{2}\right)^2 K_{ij} \quad , \tag{A-6}$$

where the matrix K_{ij} is given by

$$K = \begin{pmatrix} U^2 & \vec{U}\cdot\vec{V} \\ \vec{U}\cdot\vec{V} & V^2 \end{pmatrix} \quad ; \tag{A-7}$$

this result is given in the text as Eq.(4.5), where it constitutes the form of the monostatic-bistatic equivalence theorem for an isotropic point scatterer.

For a point dipole scatterer the situation is slightly more complicated. If we try to use Eqns.(A-4) in Eq.(5.6) to express S^B_{ij} in a form similar to S^M_{ij} except that $\hat{e}''_i$ replaces $\hat{e}_i$, we find that it cannot be done: terms of order $\beta/2$ remain in the expressions and make the equivalence impossible. This means that, in general, the monostatic-bistatic equivalence theorem does not hold true for orientable scatterers in the linear basis. But if we then use Eqns.(2.14) to transform to the circular basis, these inconvenient linear terms drop out of all the expressions, leaving the equivalent form with $\hat{e}''_i$ replacing $\hat{e}_i$ and ξ^B_n replacing ξ^M_n, good up to a term of order $\left(\frac{\beta}{2}\right)^2$. Thus, the monostatic-bistatic equivalence theorem does indeed hold true for orientable scatterers in the circular basis.

APPENDIX B

DEFINITION OF RIGIDLY CONNECTED POINT DIPOLE

Consider vector $\vec{p}$ rigidly connected to the end of vector $\vec{r}$, both vectors having constant magnitude, and vector $\vec{r}$ rotating about the origin with angular velocity $\vec{\omega}$. We know that

$$\frac{d\vec{r}}{dt} = \vec{\omega} \times \vec{r} \quad . \tag{B-1}$$

When we say that vector $\vec{p}$ is rigidly connected to vector $\vec{r}$, we intuitively mean that the relationship between $\vec{r}$ and $\vec{p}$ must remain invariant as the vectors change direction with time. This means, in the first place, that the angle between the two vectors must not change, i.e.

$$\vec{r}(t) \cdot \vec{p}(t) = \text{constant} \quad . \tag{B-2}$$

And in the second place it means that the vector $\vec{p}$ must not "twist" around vector $\vec{r}$ as they change with time: the plane defined by $\vec{r}$ and $\vec{p}$ should not rotate around $\vec{r}$. This condition is a little more difficult to express mathematically, but we shall do so in a moment.

The condition $\vec{p} \cdot \vec{p} = \text{constant}$ leads directly to the requirement that $\vec{p} \cdot \frac{d\vec{p}}{dt} = 0$, which means that $\frac{d\vec{p}}{dt}$ can always be written in the form

$$\frac{d\vec{p}}{dt} \equiv \vec{\omega}_p \times \vec{p} \qquad \text{(B-3)}$$

for some vector $\vec{\omega}_p$. Now the "no twist" condition stated above can be put mathematically by saying that $\vec{\omega}_p$ shall have no component along $\vec{r}$, i.e.

$$\vec{\omega}_p \cdot \vec{r} = 0 \qquad \text{(B-4)}$$

By differentiating Eq. (B-2) and making use of Eq. (B-1) we find that

$$\vec{r} \cdot \left(\frac{d\vec{p}}{dt} - \vec{\omega} \times \vec{p} \right) = 0 \quad ,$$

which implies that

$$\frac{d\vec{p}}{dt} \equiv \vec{\omega} \times \vec{p} + \vec{\alpha} \times \vec{r} \qquad \text{(B-5)}$$

for some vector $\vec{\alpha}$ as yet unknown. Taking the dot product with $\vec{p}$ and recalling that $\vec{p} \cdot \frac{d\vec{p}}{dt} = 0$ we see that

$$\vec{\alpha} \cdot \vec{r} \times \vec{p} = 0 \quad ,$$

which says that $\vec{\alpha}$ lies in the plane of $\vec{r}$ and $\vec{p}$, i.e.

$$\vec{\alpha} \equiv a\vec{r} - b\vec{p}$$

for some numbers a and b . Substituting this form of $\vec{\alpha}$ into

Eq. (B-5) we get

$$\frac{d\vec{p}}{dt} = (\vec{\omega} + b\vec{r}) \times \vec{p} \quad .$$

which, with definition (B-3), indicates that

$$\vec{\omega}_p \equiv \vec{\omega} + b\vec{r} \quad .$$

When this form is tested according to condition (B-4) it becomes necessary to set $b \equiv 0$, whence

$$\vec{\omega}_p \equiv \vec{\omega} \quad ,$$

or

$$\frac{d\vec{p}}{dt} = \vec{\omega} \times \vec{p} \quad . \qquad \text{(B-6)}$$

This is the desired result.

APPENDIX C

THE FUNCTION $\dot{\theta}_n$

In this appendix we shall derive and briefly discuss an expression for the form of the function $\dot{\theta}_n$ in terms of other dynamical variables. To simplify the notation, explicit mention of the subscript n will be suppressed in the intermediate steps. The starting point for this derivation is with the second and third of equations (5.10):

$$\begin{aligned} \hat{e}_1 \cdot \hat{p} &\equiv \sin\zeta \cos\theta \\ \hat{e}_2 \cdot \hat{p} &\equiv \sin\zeta \sin\theta \quad , \end{aligned} \tag{C-1}$$

whence we find at once that

$$\tan\theta(t) = \frac{\hat{e}_2(t) \cdot \hat{p}(t)}{\hat{e}_1(t) \cdot \hat{p}(t)} \quad . \tag{C-2}$$

Differentiating this expression with respect to time and rearranging terms leads to

$$\frac{d\theta}{dt} = \frac{\cos^2\theta}{(\hat{e}_1\cdot\hat{p})^2}\left[(\hat{e}_1\cdot\hat{p})(\hat{e}_2\cdot\dot{\hat{p}}) - (\hat{e}_2\cdot\hat{p})(\hat{e}_1\cdot\dot{\hat{p}}) + (\hat{e}_1\cdot\hat{p})(\dot{\hat{e}}_2\cdot\hat{p}) - (\dot{\hat{e}}_2\cdot\hat{p})(\hat{e}_1\cdot\hat{p})\right] . \tag{C-3}$$

But $\cos^2\theta/(\hat{e}_1\cdot\hat{p})^2 \equiv \mathrm{cosec}^2\zeta$, and the use of several vector identities shows that

$$(\hat{e}_1\cdot\hat{p})(\hat{e}_2\cdot\dot{\hat{p}}) - (\hat{e}_2\cdot\hat{p})(\hat{e}_1\cdot\dot{\hat{p}}) \equiv (\hat{e}_1\times\hat{e}_2)\cdot(\hat{p}\times\dot{\hat{p}}) \equiv \hat{k}\cdot\vec{\Omega} \ ,$$

where we have also used the facts that $\hat{e}_1\times\hat{e}_2 \equiv \hat{k}$, $\dot{\hat{p}} \equiv \vec{\omega}\times\hat{p}$, and $\hat{k}\cdot\vec{\omega}_A \equiv 0$. Therefore

$$\frac{d\theta_n}{dt} = \mathrm{cosec}^2\zeta_n(\hat{k}\cdot\vec{\Omega}) + \mathrm{cosec}^2\zeta_n[(\hat{e}_1\cdot\hat{p}_n)(\dot{\hat{e}}_2\cdot\hat{p}_n) - (\hat{e}_2\cdot\hat{p}_n)(\dot{\hat{e}}_1\cdot\hat{p}_n)] \ . \quad \text{(C-4)}$$

This division of $\dot{\theta}_n$ into two terms is a natural one. The first term represents the contribution to $\dot{\theta}_n$ of the motion of the target and the orientation of the individual dipole; this may be thought of as being a "dynamical" term. The second term represents the contribution to $\dot{\theta}_n$ of the change in the coordinate system with respect to which θ_n is measured, due to the motion of the polarization plane itself as $\hat{k}$ moves; this may be thought of as being a "coordinate transformation" term. Unfortunately the second term, which cannot be simplified to any significant degree, is quadratic in one of the unknowns: $\hat{p}_n$. Therefore it seems very probable that the information about the target motion and about the scatterer orientation which is contained in equation (C-4) cannot be disentangled and extracted from the equation. Thus the knowledge of $\dot{\theta}_n$ which can be found by comparing frequency shifts of the diagonal terms of the transformed scattering matrix will have to suffice in itself and not as a prelude to more useful information about the target.

REFERENCES

1. N.M. Tomljanovich, H.S. Ostrowsky, J.F.A. Ormsby, "Narrowband Interferometer Imaging," ESD-TR-68-274, The MITRE Corporation, Bedford, Mass., 6 November 1967.

2. H.S. Ostrowsky, "Background for Narrowband Interferometry I. Isotropic Point Scatterers," ESD-TR-68-275, 11 December 1967.

3. M.R. Weiss, "The Doppler Map of an Edge," ESD-TR-68-276, 12 April 1968.

4. J.L. Altman, R.H.T. Bates, E.N. Fowle, "Introductory Notes Relating to Electromagnetic Inverse Scattering," The MITRE Corporation SR-121, September 1964.

5. S.H. Bickel, "Some Invariant Properties of the Polarization Scattering Matrix," The MITRE Corporation MTP-2, July 1965.

6. S.H. Bickel & J.F.A. Ormsby, "Error Analysis, Calibration, and the Polarization Scattering Matrix," The MITRE Corporation, MTP-3, July 1965.

7. S.H. Bickel & R.H.T. Bates, "Effects of Magnetic-Ionic Propagation on the Polarization Scattering Matrix," The MITRE Corporation, MTP-4, July 1965.

8. J.D. Kraus, Antennas, New York, McGraw Hill (1950), P.471.

Security Classification

DOCUMENT CONTROL DATA - R & D

(Security classification of title, body of abstract and indexing annotation must be entered when the overall report is classified)

1. ORIGINATING ACTIVITY *(Corporate author)*	2a. REPORT SECURITY CLASSIFICATION
The MITRE Corporation, Bedford, Massachusetts	UNCLASSIFIED
	2b. GROUP

3. REPORT TITLE

NARROWBAND INTERFEROMETRY AND THE POLARIZATION SCATTERING MATRIX

4. DESCRIPTIVE NOTES *(Type of report and inclusive dates)*

N/A

5. AUTHOR(S) *(First name, middle initial, last name)*

H. S. Ostrowsky

6. REPORT DATE	7a. TOTAL NO. OF PAGES	7b. NO. OF REFS
December 1968	74	8

8a. CONTRACT OR GRANT NO.	9a. ORIGINATOR'S REPORT NUMBER(S)
AF 19(628)-5165	ESD-TR-68-401
b. PROJECT NO. 4966	
c.	9b. OTHER REPORT NO(S) *(Any other numbers that may be assigned this report)*
d.	MTR-743

10. DISTRIBUTION STATEMENT

This document has been approved for public release and sale; its distribution is unlimited.

11. SUPPLEMENTARY NOTES	12. SPONSORING MILITARY ACTIVITY
N/A	Space Defense and Command System Program Office, Electronic Systems Division, Air Force Systems Command, L. G. Hanscom Field, Bedford, Massachusetts

13. ABSTRACT

Two previous papers have described the concept and some of the applications of Narrowband Interferometry, using monostatic and multistatic radars (at small bistatic angles) to obtain two and three dimensional "images" of targets in terms of their scattering centers. The method involves taking finite Fourier transforms of measured narrowband amplitude and phase data to resolve individual scattering centers in "Doppler" at each radar site.

The present paper extends these methods in two directions. The class of scattering centers considered is widened to include not only isotropic point scatterers as before but also point dipoles, as representatives of orientable scattering centers. The theory is broadened to involve the Polarization Scattering Matrix, so that the polarization behavior of the individual resolved scatterers can be determined as aids to their recognition.

DD FORM 1 NOV 65 1473

Security Classification

14. KEY WORDS	LINK A		LINK B		LINK C	
	ROLE	WT	ROLE	WT	ROLE	WT
INTERFEROMETRY ELECTROMAGNETIC SCATTERING						